

Exact Solutions of the Einstein-Maxwell Field Equations in Paraboloidal Geometry Using Chaplygin Equation of State



By

Aqsa Hafeez

(Registration No: 00000402911)

Supervisor: Prof. Tooba Feroze

A thesis submitted to the National University of Sciences and Technology, Islamabad,

in partial fulfillment of the requirements for the degree of

Master of Science in

Mathematics

School of Natural Sciences

National University of Sciences and Technology (NUST)

Islamabad, Pakistan

(2024)

77-1-
MISSING

THESIS ACCEPTANCE CERTIFICATE

Certified that final copy of MS thesis written by Aqsa Hafeez (Registration No 00000402911), of School of Natural Sciences has been vetted by undersigned, found complete in all respects as per NUST statutes/regulations, is free of plagiarism, errors, and mistakes and is accepted as partial fulfillment for award of MS/M.Phil degree. It is further certified that necessary amendments as pointed out by GEC members and external examiner of the scholar have also been incorporated in the said thesis.

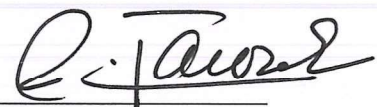
Signature: 

Name of Supervisor: Prof. Tooba Feroze

Date: 05/09/2024

Signature (HoD): 


Date: 5/9/2024

Signature (Dean/Principal): 

Date: 05.09.2024

National University of Sciences & Technology**MS THESIS WORK**

We hereby recommend that the dissertation prepared under our supervision by: Aqsa Hafeez, Regn No. 00000402911 Titled Exact Solution to Einstein-Maxwell Field Equations in Paraboloidal Geometry Using Chaplygin's Equation of State be Accepted in partial fulfillment of the requirements for the award of MS degree.

Examination Committee Members1. Name: PROF. MUBASHER JAMILSignature: 2. Name: DR. MUHAMMAD ALI PARACHASignature: Supervisor's Name PROF. TOOBA FEROZESignature: 


 Head of Department

5/9/2024

 Date
COUNTERSIGNEDDate: 05.09.2024


 Dean/Principal

DEDICATION

بِسْمِ اللَّهِ الرَّحْمَنِ الرَّحِيمِ

In the name of **Allah**, the most beneficent, Merciful and Compassionate, I am profoundly thankful to **Allah Almighty** for His countless blessings and guidance that brighten-up my life.

This thesis is dedicated to my family, whose continuous support and encouragement have been my foundation throughout this journey.

ACKNOWLEDGEMENTS

Above all, I want to express my sincere gratitude to **Allah** for providing me the courage, determination, and wisdom needed to successfully complete this research. I would like to convey my sincerest gratitude to my supervisor, **Prof. Tooba Feroze**, for their immense guidance, insightful contributions, and continuous support. Your knowledge and support have been crucial in guiding and completing this research. I am sincerely grateful to my family for their unconditional love, patience, and encouragement. To my parents, thank you for always believing in me and providing a foundation for my academic goals. To my siblings, thank you for your continuing support and understanding during this challenging time. I also wish to thank my friends (specially **Tayyaba Ibrahim**) for their companionship, encouragement, and intriguing talks that have enriched my understanding and kept me motivated. Finally, I would like to appreciate the teachers and staff of the SNS, whose assistance and resources have been important to my research.

Abstract

This thesis investigates a charged anisotropic stellar model in paraboloidal geometry, using the Chaplygin equation of state. We develop a new solution to Einstein's field equations that investigates the interaction of electromagnetic fields and, anisotropic pressures. This solution satisfies all physically admissible conditions. This model also fulfills all stability conditions, including hydrostatic equilibrium, the adiabatic index and, Abreu's criterion. By assuming the values of parameters, we can develop detailed profiles of the compact stars in our model. These profiles show how density, pressure, and electric field vary throughout the star.

Contents

ABSTRACT	II
LIST OF TABLES	IV
LIST OF FIGURES	VI
1 Introduction	1
1.1 General Relativity: Principles And Foundations	1
1.1.1 Role Of Electrodynamics	1
1.1.2 Special Relativity	2
1.1.2.1 Equivalence Principle	3
1.1.2.2 Principal of General Covariance	4
1.2 Tensors	4
1.2.1 Metric Tensor	5
1.2.2 Curvature Tensor	6
1.2.3 The Einstein Tensor	7
1.2.4 The Maxwell Tensor	8
1.3 Spacetime Curvature And Geodesics	9
1.4 The Maxwell Equation in Relativity	9
1.5 The Energy Momentum Tensor	10
1.6 The Einstein Field Equation	11
2 Exact Solutions for Anisotropic Compact Stars in General Relativity	13
2.1 Exact Solutions	13
2.2 Compact Objects	14
2.2.1 White Dwarfs	14
2.2.2 Neutron Stars	14
2.2.3 Black Holes	14
2.3 Exploring Notable Exact Solutions of Einstein's Field Equations	15
2.3.1 Schwarzschild Solution	15
2.3.2 Reissner-Nordstrom Solution	17
2.4 Admissible Conditions for Compact Objects	18
2.5 Review of Model of a Static Spherically Symmetric Anisotropic Fluid Dis- tribution in Paraboloidal Spacetime Admitting a Polytopic Equation of State	19
2.5.1 Polytopic Models	20
2.5.2 Discussion	21

3	Charged Anisotropic Model with Chaplygin's Equation of State	23
3.1	Chaplygin's Equation of State	23
3.2	Exact Solutions with Chaplygin's Equation of State	24
3.2.1	Chaplygin's Model	25
3.2.2	Boundary Conditions	26
3.2.3	Physical Conditions	27
3.2.4	Stability Conditions	36
4	Conclusion	42
	BIBLIOGRAPHY	43

List of Figures

3.1	Graph of Metric Potentials are plotted for the constants: $L = 1.8$, $a = 1.08977$, $\zeta = 0.01$, and $\alpha = 0.06184373$ with respect to r	27
3.2	Graph of Electric Field Intensity is plotted for the constants: $L = 1.8$, $a = 1.08977$, $\zeta = 0.01$, and $\alpha = 0.06184373$ with respect to r	28
3.3	Graph of Energy Density is plotted for the constants: $L = 1.8$, $a = 1.08977$, $\zeta = 0.01$, and $\alpha = 0.06184373$ with respect to r	28
3.4	Graph of Pressures are plotted for the constants: $L = 1.8$, $a = 1.08977$, $\zeta = 0.01$, and $\alpha = 0.06184373$ with respect to r	29
3.5	Graph of Pressure-Density Ratios are plotted for the constants: $L = 1.8$, $a = 1.08977$, $\zeta = 0.01$, and $\alpha = 0.06184373$ with respect to r . The green curve represents the ratio of radial pressure to energy density and the blue dashed curve represents the ratio of tangential pressure to energy density.	30
3.6	Graph of Energy Tensor Trace is plotted for the constants: $L = 1.8$, $a = 1.08977$, $\zeta = 0.01$, and $\alpha = 0.06184373$ with respect to r	30
3.7	Graph of Anisotropic Factor is plotted for the constants: $L = 1.8$, $a = 1.08977$, $\zeta = 0.01$, and $\alpha = 0.06184373$ with respect to r	31
3.8	Graph of Density Gradient is plotted for the constants: $L = 1.8$, $a = 1.08977$, $\zeta = 0.01$, and $\alpha = 0.06184373$ with respect to r	33
3.9	Graph of Radial Pressure Gradient is plotted for the constants: $L = 1.8$, $a = 1.08977$, $\zeta = 0.01$, and $\alpha = 0.06184373$ with respect to r	33
3.10	Graph of Tangential Pressure Gradient is plotted for the constants: $L = 1.8$, $a = 1.08977$, $\zeta = 0.01$, and $\alpha = 0.06184373$ with respect to r	34
3.11	Graph of Mass is plotted for the constants: $L = 1.8$, $a = 1.08977$, $\zeta = 0.01$, and $\alpha = 0.06184373$ with respect to r	35
3.12	Graph of compactness Factor is plotted for the constants: $L = 1.8$, $a = 1.08977$, $\zeta = 0.01$, and $\alpha = 0.06184373$ with respect to r	35
3.13	Graph of Surface and Gravitational Redshifts are plotted for the constants: $L = 1.8$, $a = 1.08977$, $\zeta = 0.01$, and $\alpha = 0.06184373$ with respect to r	36
3.14	Graph of Radial and Tangential Speed of Sounds are plotted for the constants: $L = 1.8$, $a = 1.08977$, $\zeta = 0.01$, and $\alpha = 0.06184373$ with respect to r	38
3.15	Graphs of Energy Conditions are plotted for the constants: $L = 1.8$, $a = 1.08977$, $\zeta = 0.01$, and $\alpha = 0.06184373$ with respect to r	39
3.16	Graph of Radial and Tangential Adiabatic Index are plotted for the constants: $L = 1.8$, $a = 1.08977$, $\zeta = 0.01$, and $\alpha = 0.06184373$ with respect to r	40

3.17 Graph of Forces is plotted for the constants: $L = 1.8$, $a = 1.08977$, $\zeta = 0.01$, and $\alpha = 0.06184373$ w.r.t r . Where, the green curve depicts the anisotropic force, the blue dashed curve represents the hydrostatic force, the brown dashed curve represents the electric force, and the red doted curve represents the gravitational force. 41

Chapter 1

Introduction

1.1 General Relativity: Principles And Foundations

The concept of space and time has been studied by several scientists. Aristotle, in the fourth century BC, approached this from the standpoint that space is comparable to the substance of matter and time to the series of events. He came to the conclusion that time is the potentiality of the motion of matter [1]. The discoveries and significant contributions of Galileo Galilei and especially Isaac Newton caused this word's meaning to change over the 17th and 18th centuries.

In 1632, Galileo Galilei provided a direct connection between past theories by introducing the concept of relativity, which stated that the laws of motion are the same in all inertial frames of reference, regardless of the observers' relative positions or motions. He articulated the idea that every rule of physics is equivalent in any inertial reference frame.

Newtonian mechanics also gave rise to new theories regarding the laws of motion, gravity, and the absoluteness of space and time. Newton's laws of motion and universal gravitation became the cornerstones of classical mechanics following the publication of his Principia in 1687. From the motion of planets to the behavior of objects on Earth, Newton's work established a mathematical framework that explained a wide range of physical phenomena.

After Isaac Newton's work in the late 17th century, the 18th and early 19th centuries witnessed significant developments in the study of natural phenomena. During the 18th century, also referred to as the Age of Enlightenment, scientists like Benjamin Franklin, Hans Christian Ørsted, and Michael Faraday made significant advancements in mechanics, astronomy, and the early fields of electricity and magnetism. These paved the way for Maxwell's development of Maxwell's equations in the middle of the 19th century, which united electricity, magnetism, and light and fundamentally transformed our knowledge of physics to create modern theories.

1.1.1 Role Of Electrodynamics

Maxwell discussed the conditions demonstrating the characteristics of electricity, magnetism, and light into a single framework known as electromagnetic field in 1864 [5]. Electric charge (Q) and current (I) are the two primary sources of the electromagnetic field, fixed charges provide an electric field, and moving charges produce a magnetic field. To quantify the effects of fields, Maxwell's equations use charge and current densities [6].

The equations split up in two pairs the "source equations"

$$\nabla \cdot \mathbf{E} = \rho, \tag{1.1}$$

$$\nabla \times \mathbf{B} - \partial_t \mathbf{E} = \mathbf{j}, \tag{1.2}$$

and the "internal equations"

$$\nabla \cdot \mathbf{B} = 0, \tag{1.3}$$

$$\nabla \times \mathbf{E} - \partial_t \mathbf{B} = 0, \tag{1.4}$$

where \mathbf{E} is the electric field, \mathbf{B} is the magnetic field, ∂ is the partial derivative, ρ is the electric charge density, and \mathbf{j} is the current density [7]. Since these equations were not Galilean-invariant, Maxwell's theory of electromagnetism could not be applied, and it was only effective in the limit $|v| \ll c$, where v is velocity of moving object and c is speed of light. One of the main questions about incompatibility was brought up by Michelson and Morley's unsuccessful attempt to determine the speed of the earth about the ether in 1887. This gives rise to two possible outcomes: either the ether is physically bonded to the earth, which would cause further issues, or there is no ether at all, in which case the speed of light would be the basic quantity of the medium [8].

Furthermore, energy is thought to likewise exist in the form of waves and to have existed continuously in waves. The contradiction associated with the wave-based theory, however, suggested that the energy conveyed was, in reality, unlimited. The previously established law of thermodynamics was called into doubt by these proven advances. Planck, therefore, clarified the remarkable results related to light and pioneered theories that light may consist of wave particles or quanta, rather than just waves [3]. However, there was still no satisfactory explanation until Einstein's suggestion came to fruition, which completely eliminated any frameworks for reference about space and time and significantly undermined the ether theories.

1.1.2 Special Relativity

With his four groundbreaking publications in 1905—The Photoelectric Effect, the Equivalency of mass and energy, the special relativity theory presented in the paper "On the Electrodynamics of Moving Bodies," and his work on "Brownian Motion" Einstein revolutionized physics in an instant [9]. He provided evidence that there is no such thing as universal space and that nothing can move faster than the speed of light. His findings meant that space and time were combined to form a single entity known as space-time, with all measurements being related to the observer's position and speed. The main focus of Einstein's thought was electrodynamics. He deduced that a special theory of relativity was necessary to satisfy Maxwell's condition for electromagnetic.

The two postulates of the special theory of relativity are [2]

1. The rules of physics take on the same shape, and all observers are equal in all inertial reference frames.
2. Observers in all the frames of the inertial reference will agree to measure equal speed of light from any light source, irrespective of the motion of the observer.

This theory has several ramifications that include lengths being contracted, time being dilated, and mass being increased.

Minkowski in 1907 then came up with a way of describing events in the universe, which he described as the four-dimensional hyperspace event or spacetime event. This required

the new values defining the position of the point and time as well as the transformation equations that became known as the Lorentz transformations in the same way as the Galilean transformations were used in the theory of classical mechanics. These transformations are called linear coordinate transformations and act like two frames that are moving at a constant speed to each other. The Minkowski line element represents the square of the infinitesimal interval between two events (ct, x) and $(ct + c dt, x + dx)$ that are infinitesimally separated in spacetime (without acceleration). This interval remains invariant under Lorentz transformations [2]

$$ds^2 = -c^2 dt^2 + dx^2 + dy^2 + dz^2. \quad (1.5)$$

The fact that the Maxwell equations remain invariant under these changes is one of their main contributions to the special theory of relativity. However, this was not the end since shortly after this ground-breaking study, Einstein started to question gravity and if Newton's theory of gravitation, which states that gravity works as an attracting force when two large objects meet, is entirely consistent with his theory or not, given that the notion of gravitational propagation seemed a little strange when seen within the context of special relativity. The most significant consequences of the theory of special relativity, which has been experimentally tested and validated are:

1. **Time Dilataion:** Objects, in motion experience time passing slower relative to observer.
2. **Length Contraction:** When compared to an observer at rest, objects in motion look shorter in the direction in which they are moving.
3. **Mass Variation:** An object's mass increases with its velocity according to special relativity. This depends on the object's velocity and is commonly referred to as relativistic mass.

Over the next decade, these ideas gradually solidified, into what would form the foundation of the General Theory of Relativity or GR as Einstein presented in 1915 [10]. In contrast to GR, Newton's law explained the reaction to gravity as pure math through the basic equations of physics, but GR concerned itself with the consequences of gravity as shaping the structure of spacetime itself, asserting that spacetime is not just an unchanging canvas with objects exerting influence and thereby changing its geometry. Thus, in the 'grand unified' theory called GR, forces are not as in Newtonian physics; they are replaced by the warping of space and time. This theory is based on the following premises:

1. Equivalence Principle
2. Principle of General Covariance

1.1.2.1 Equivalence Principle

The equivalence principle is a fundamental concept in GR. It consists of two principles, the weak equivalence principle, first observed by Galileo Galilei, which states that the composition of an object does not impact its free fall in a gravitational field, and the Einstein equivalence principle, developed by Albert Einstein, which extends this idea to assert that the laws of physics in a freely falling frame are identical to those in special relativity. This implies that gravity results from spacetime curvature caused by matter and energy [12].

1. **Weak equivalence Principle:** According to the weak equivalency principle, an object's interior composition and structure has no bearing on how it falls freely in a grav-

itational field. Put another way, regardless of their mass or internal makeup, all objects fall at the same rate in the same gravitational field. Galileo Galilei initially noticed this idea, sometimes referred to as the universality of free fall, in his well-known experiments with falling objects.

2. Einstein Equivalence Principle: A generalization of the weak equivalency concept is the Einstein equivalence principle. It asserts that all of the rules of physics, not simply those pertaining to gravity, assume their special relativistic forms in a freely falling reference frame. Stated differently, local experiments cannot discriminate between a uniformly accelerated reference frame and a uniform gravitational field.

The EEP suggests that instead of being a force in the conventional sense, gravity is a result of spacetime's curvature brought on by the presence of matter and energy. The shortest pathways, or geodesics, in curved spacetime, are followed by objects, and their velocity is determined by this curvature.

1.1.2.2 Principal of General Covariance

A key idea in GR is the concept of general covariance, which says the following: "The laws of physics must be specified in tensorial form as they remain constant regardless of the coordinate transformations used." In simpler words, general covariance indicates that the principles of physics are expressed in a way that is independent of any particular choice of coordinates, making the mathematical explanations of physical processes universally applicable [7].

1.2 Tensors

Tensors are mathematical entities that have transformation features that fully characterize them in their corresponding coordinate systems. Since tensor formalism provides the language needed to explain how quantities transform under coordinate transformation since they are true in all systems, it is studied in relativity to get a deeper understanding of the geometry of spacetime. Fundamentally, dual vectors and vectors are generalized into tensors. If \mathbf{T} is (r, s) tensor then in component notation, it is written as

$$\mathbf{T} = T_{j_1 \dots j_s}^{i_1 \dots i_r} \hat{e}_{i_1} \otimes \dots \otimes \hat{e}_{i_r} \otimes \hat{v}^{j_1} \otimes \dots \otimes \hat{v}^{j_s}, \quad (1.6)$$

where

$$\hat{e}_{i_1} \otimes \dots \otimes \hat{e}_{i_r} \otimes \hat{v}^{j_1} \otimes \dots \otimes \hat{v}^{j_s}, \quad (1.7)$$

is the basis of (r, s) tensor, given by the tensor product of vectors and dual vectors. Components of covariant and contravariant tensors with all upper and lower indices, respectively, may also be determined in this way.

The transformation law for the components of mixed tensor is defined as

$$T_{j'_1 \dots j'_s}^{i'_1 \dots i'_r} = T_{j_1 \dots j_s}^{i_1 \dots i_r} \frac{\partial x^{i'_1}}{\partial x^{i_1}} \dots \frac{\partial x^{i'_r}}{\partial x^{i_r}} \frac{\partial x^{j_1}}{\partial x^{j'_1}} \dots \frac{\partial x^{j_s}}{\partial x^{j'_s}}. \quad (1.8)$$

While the product of two tensors provided by its components, whose upper and lower indices include of all upper and lower indices of the original tensor components, is valid, basic operations like addition and subtraction are only valid for tensors if they have the

same rank and type. It is expressed as follows

$$T_c^{ab} = U_c^{ab} \pm V_c^{ab}, \quad (1.9)$$

$$T_{ef}^{abc} = U_e^{ab} V_f^c. \quad (1.10)$$

Tensor would not hold the transformation rules if contraction were not the sum of an upper and a lower index (of the same kind).

As an example consider

$$S_c^{ab} = T_{cd}^{adb}. \quad (1.11)$$

Given a tensor, its symmetric and skew-symmetric parts are defined as follows

$$T_{(i_1 \dots i_n)} = \frac{1}{n!} \left(T_{i_1 \dots i_n} + \sum \text{ over permutations of indices } i_1 \dots i_n \right), \quad (1.12)$$

$$T_{[i_1 \dots i_n]} = \frac{1}{n!} (T_{i_1 \dots i_n} + \text{alternating sum over permutations of indices } i_1 \dots i_n). \quad (1.13)$$

1.2.1 Metric Tensor

A key concept in relativity is the metric tensor, which is particularly important for studying the geometric characteristics of manifolds in any finite number of dimensions. It is necessary to define parameters inside the manifold, such as curvature and distance. Its components are defined in terms of basis vector e_a

$$g_{ab} = e_a \cdot e_b. \quad (1.14)$$

Since the dot product $e_a \cdot e_b = e_b \cdot e_a$, this implies the symmetry of the second-rank tensor, i.e.

$$g_{ab} = g_{ba}. \quad (1.15)$$

The metric tensor is also defined as the square of infinitesimal distance between two points $R(x_a)$ and $S(x_a + dx_a)$ on a manifold given as

$$ds^2 = g_{ab} dx^a dx^b. \quad (1.16)$$

The tensor g^{ab} is the inverse metric of g_{ab} since $g^{ab} g_{bc} = \delta_c^a$. where δ_c^a is Kronecker delta. The metric determinant g is the determinant of the $n \times n$ symmetric non-degenerate matrix, i.e.

$$g = \det(g_{ab}).$$

Properties

1. It is used in causing the index to rise or fall.
2. The law of transformation for second rank tensor (g_{ab}) can be easily figured out from equation (1.8).
3. The condition $g_{ab;c} = 0$ implies that the metric tensor is consistent with the covariant derivative, indicating that the metric is conserved when differentiating along any direction. This condition is crucial in defining a link or a technique to differentiate tensors in curved spacetime.

1.2.2 Curvature Tensor

The general theory of relativity revealed a deep relationship between gravity and accelerated observers. It is suggested that the existence of mass is what causes spacetime to distort. These masses cause spacetime to curve, as opposed to having a flat structure, this curvature is explained by the Riemann tensor.

The generalization of partial derivative ∂ , for a curved spacetime, is the covariant derivative ($;$). The components of a tensor of rank $(1, 1)$'s covariant derivative, for instance, are defined as

$$A^a_{b;c} = A^a_{b,c} + \Gamma^a_{bd}A^d_c - \Gamma^d_{cb}A^a_d. \quad (1.17)$$

Here, Γ^a_{bc} , the Christoffel symbol, is defined as

$$\Gamma^a_{bc} = \frac{1}{2}g^{ad} \left(\frac{\partial g_{cd}}{\partial x^b} + \frac{\partial g_{bd}}{\partial x^c} - \frac{\partial g_{bc}}{\partial x^d} \right). \quad (1.18)$$

The Christoffel symbol is symmetric, i.e. $\Gamma^a_{bc} = \Gamma^a_{cb}$.

In contrast to partial derivatives, which are commutative (meaning that the differentiation order is irrelevant), covariant derivatives are not necessarily commutative since spacetime is curved. This non-commutativity is what give rise to the Riemann curvature tensor.

$$A^a_{;d;c} - A^a_{;c;d} = A^a_{;d,c} + \Gamma^a_{ce}A^e_{;d} - \Gamma^e_{dc}A^a_{;e} - A^a_{;c,d} - \Gamma^a_{de}A^e_{;c} + \Gamma^e_{cd}A^a_{;e}, \quad (1.19)$$

$$A^a_{;d;c} - A^a_{;c;d} = ((\Gamma^a_{bd})_{,c} - (\Gamma^a_{bc})_{,d} + \Gamma^a_{ce}\Gamma^e_{db} - \Gamma^a_{de}\Gamma^e_{cb}) A^b. \quad (1.20)$$

$$A^a_{;d;c} - A^a_{;c;d} = R^a_{bcd}A^b. \quad (1.21)$$

where

$$R^a_{bcd} = (\Gamma^a_{bd})_{,c} - (\Gamma^a_{bc})_{,d} + \Gamma^a_{ce}\Gamma^e_{db} - \Gamma^a_{de}\Gamma^e_{cb}. \quad (1.22)$$

Non-commutativity of covariant derivative characterizes the deviation from flat spacetime, which is expressed by the Riemann curvature tensor R^a_{bcd} . In simple terms

- If $R^a_{bcd} = 0$, the geometry is flat, meaning spacetime is not curved.
- If $R^a_{bcd} \neq 0$, the geometry is curved, reflecting the influence of mass and energy on the structure of spacetime.

R^a_{bcd} can be transformed into covariant tensor form by using the transformation

$$R_{abcd} = g_{ae}R^e_{bcd}, \quad (1.23)$$

In general $R^a_{bcd} \neq R_{abcd}$. The components in explicit form, by performing some algebra, can be written as

$$R_{abcd} = \frac{1}{2} (g_{da,bc} + g_{bc,da} - g_{bd,ac} - g_{ca,bd}) + g_{pe} (\Gamma^e_{da}\Gamma^p_{cb} - \Gamma^e_{ca}\Gamma^p_{db}). \quad (1.24)$$

The properties of the curvature tensor are as follows

1. It is skew-symmetrical either in the final two indices order or in the first two indices order.

$$R_{abcd} = -R_{bacd}, \quad R_{abcd} = -R_{abdc}. \quad (1.25)$$

2. It is symmetric if the first two pairs of indices are swapped with the last two

$$R_{abcd} = R_{cdab}. \quad (1.26)$$

3. It satisfies Bianchi's identities of first and second kind given as

$$R^a{}_{[bcd]} = R^a{}_{bcd} + R^a{}_{dbc} + R^a{}_{cdb} = 0, \quad (1.27)$$

$$R^a{}_{p[bc;d]} = R^a{}_{pbc;d} + R^a{}_{pdc;b} + R^a{}_{pcd;b} = 0. \quad (1.28)$$

One may obtain the components of Ricci tensor by contracting the components of the Riemann tensor.

$$R_{ab} = R^c{}_{acb}, \quad (1.29)$$

The Ricci tensor depends on the metric tensor and is known to be a symmetric tensor. Likewise, the Ricci scalar, also known as the curvature scalar, is the trace of the Ricci tensor as shown below

$$R = g^{ab}R_{ab}. \quad (1.30)$$

Ricci scalar has the interesting property that it does not depend on the particular coordinate system used to study the kind of singularity which may exist at some point. The singularity is either coordinated or essential, the first one appears when there is a bad choice of coordinates and could be removed, and the second is tied up with some problems in geometry, which are impossible to avoid. The following invariant are used to determine the nature of singularities either coordinate or essential.

$$R_1 = R, \quad (1.31)$$

$$R_2 = R^{ab}{}_{cd}R^{cd}{}_{ab}, \quad (1.32)$$

$$R_3 = R^{ab}{}_{cd}R^{cd}{}_{ef}R^{ef}{}_{ab}, \quad (1.33)$$

$$R_4 = R^{ab}{}_{cd}R^{cd}{}_{ef}R^{ef}{}_{gh}R^{gh}{}_{ab}. \quad (1.34)$$

.

1.2.3 The Einstein Tensor

The symmetric, linear, and divergence-free function of the curvature is provided by the Einstein tensor. Using the second form of Bianchi identity given by equation (1.27)

$$R^a{}_{pac;d} + R^a{}_{pda;c} + R^a{}_{pcd;a} = 0. \quad (1.35)$$

Substituting $R^a{}_{pac} = R_{pc}$ and $R^a{}_{pda} = -R^a{}_{pad} = -R_{pd}$ into equation (1.21)

$$R_{pc;d} - R_{pd;c} - R^a{}_{pcd;a} = 0, \quad (1.36)$$

Multiplying the above equation by g^{pc} gives

$$R^c{}_{c;d} - R^c{}_{d;c} - R^a{}_{d;a} = 0, \quad (1.37)$$

$$R_{;d} - R^a{}_{d;a} - R^a{}_{d;a} = 0, \quad (1.38)$$

$$\frac{1}{2}R_{;d} - R^a_{d;a} = 0, \quad (1.39)$$

Carrying out some contractions in equation (1.39) by multiplying with δ_a^a reduces to

$$\left(R^a_d - \frac{1}{2}\delta^a_d R \right)_{;a} = 0, \quad (1.40)$$

where

$$G^a_d = R^a_d - \frac{1}{2}\delta^a_d R. \quad (1.41)$$

Here, equation (1.41) provides the Einstein tensor G in component form, where equation (1.40) suggests that $G^a_{d;a} = 0$. The covariant form of the Einstein equation is

$$G_{ab} = R_{ab} - \frac{1}{2}Rg_{ab}. \quad (1.42)$$

which is symmetric and divergence-free.

1.2.4 The Maxwell Tensor

The Maxwell tensor, sometimes referred to as the electromagnetic field tensor, is constructed by first defining the skew-symmetric tensor $F = F_{ab}\mathbf{e}^a \otimes \mathbf{e}^b$ and the four-vector potential \mathbf{A} .

$$A_a = (\phi, \mathbf{A}), \quad (1.43)$$

$$F_{ab} = \partial_a A_b - \partial_b A_a. \quad (1.44)$$

Here, \mathbf{A} represents the 3-vector potential and ϕ is the scalar potential. In terms of ϕ and \mathbf{A} , the electric and magnetic fields become

$$\mathbf{E} = -\nabla\phi - \partial_t\mathbf{A}, \quad (1.45)$$

$$\mathbf{B} = \nabla \times \mathbf{A}. \quad (1.46)$$

We define $F_{0i} = -E_i$ and $F_{ij} = \varepsilon_{ijk}B^k$ by using equations (1.45)–(1.47), where $i, j, k = 1, 2, 3$, and ε_{ijk} is the Levi-Civita symbol (0, 3) defined as

$$\varepsilon_{ijk} = \begin{cases} +1 & \text{if } (i, j, k) \text{ is an even permutation of } (1, 2, 3) \\ -1 & \text{if } (i, j, k) \text{ is an odd permutation of } (1, 2, 3) \\ 0 & \text{if any two indices are equal} \end{cases}. \quad (1.47)$$

The covariant components of the electromagnetic field tensor are

$$F_{ab} = \begin{pmatrix} 0 & E_1 & E_2 & E_3 \\ -E_1 & 0 & B_3 & -B_2 \\ -E_2 & -B_3 & 0 & B_1 \\ -E_3 & B_2 & -B_1 & 0 \end{pmatrix}. \quad (1.48)$$

The contravariant form of the electromagnetic field tensor can be obtained as $F^{ab} = g^{ac}g^{bd}F_{cd}$ [14].

1.3 Spacetime Curvature And Geodesics

A key concept in GR, spacetime curvature, describes how mass and energy cause the four-dimensional structure of spacetime to distort. The motion of objects in spacetime is directly influenced by this curvature. The metric tensor provides a mathematical description of the geometry of spacetime. This tensor defines the interweaving of time and space by giving a means of measuring lengths and angles in curved spacetime. A key concept in GR, spacetime curvature, describes how mass and energy cause the four-dimensional structure of spacetime to distort. The motion of objects in spacetime is directly influenced by this curvature. The metric tensor provides a mathematical description of spacetime's curvature. This tensor defines the interweaving of time and space by giving a means of measuring lengths and angles in curved spacetime. The Riemann curvature tensor is used by GR to represent the precise curvature at each location in spacetime. The degree to which spacetime is bent around a mass is measured by this tensor [11].

Geodesics: The pathways that particles and light beams take in spacetime when they are traveling just due to gravity and not under the influence of any other forces are known as geodesics. These are the flat space analogs of straight lines in GR. Geodesics are the naturally occurring paths that particles take in curved spacetime.

1. Moving through spacetime, particles essentially "choose" the path requiring the least amount of effort, which in the case of curved spacetime is the geodesic.

2. For example, a planet's orbit around a star may be thought of as a geodesic path inside the curved spacetime that the star's mass has formed. These paths are mathematically described by the geodesic equation, which is derived from the Euler–Lagrange equation. It connects the motion of particles across spacetime to its curvature [7]. This concept substitutes the geometric attribute of curvature for the traditional conception of forces operating at a distance, such as gravity. Because of this, an object traveling in a gravitational field does so by adhering to the curved spacetime geometry that the universe's mass and energy have determined.

1.4 The Maxwell Equation in Relativity

Currently, the primary objective is to observe electromagnetism in relation to relativity. To demonstrate the necessity of converting equations (1.1)-(1.4) into tensor notation, the electromagnetic field tensor, represented by equation (1.48), and the four-vector j^a , defined as $j^a = (\rho, \mathbf{j})$, are used. Consequently, the set of conventional Maxwell equations in tensor form is simplified to the following two equations:

$$\partial_b F_{ab} = j_a, \tag{1.49}$$

$$\partial_b F_{ac} = 0. \tag{1.50}$$

The source equation (1.50), which may be expressed in coordinate invariant (arbitrary coordinates) ways, is valid in Minkowski space (inertial coordinates).

$$F_{;b}^{ab} = j^a, \tag{1.51}$$

Conversely, since $F_{ac;b} = \partial_b F_{ac} = 0$ does not change, the internal equation (1.50), which is subject to the continuity equation, is satisfied automatically. These covariant tensor

equations hold true for all coordinate systems if they hold true for only one.

1.5 The Energy Momentum Tensor

The energy-momentum tensor \mathbf{T} plays a key role in constructing gravitational field equations. It is related to Einstein's tensor \mathbf{G} and describes the distribution and motion of matter and energy in spacetime.

The conservation equation of energy and momentum is given as

$$T^{ab};_b = 0. \quad (1.52)$$

For flat spacetime, this becomes

$$\partial_b T^{ab} = 0. \quad (1.53)$$

1. Energy Momentum Tensor for a Dust: The most well-known energy-momentum tensor is that of "dust," whose distribution is defined by the matter density ρ and the four-velocity u^a of the fluid at a given coordinate x^a as

$$T^{ab} = \rho u^a u^b. \quad (1.54)$$

2. Energy Momentum Tensor for a Perfect Fluid: A perfect fluid is characterized by the absence of viscosity and heat conduction in the inertial reference frame, as well as forces between the particles [11]. It can be characterized by adding scalar pressure p along with energy density ρ and flow vector u^a as

$$T^{ab} = (\rho + p)u^a u^b + p g^{ab}. \quad (1.55)$$

where g^{ab} is the component of the metric tensor of spacetime.

T^{ab} is a symmetric rank-2 energy-momentum tensor and note that a perfect fluid becomes dust if $p \rightarrow 0$.

The physical meanings components and a detailed description are given as [11]:

- T^{00} represents the energy density ρ .
- T^{i0} is the flow of the i^{th} component of momentum, called the momentum density (momentum per unit volume).
- T^{0i} is the flow of energy across the surface x^i , called the energy flux.
- T^{ij} is the flow of the i^{th} component of momentum crossing the interface in the j^{th} direction, which gives the force per unit area called stress.

For this reason, the stress-energy tensor is another name for the energy-momentum tensor. The ideal fluid tensor is an alternative representation of the energy-momentum tensor that has to do with matter dispersion.

4. The Maxwell energy-momentum tensor: The Maxwell energy-momentum tensor is given as:

$$T^{ab} = F^{ac} F_c^b - \frac{1}{4} g^{ab} F^{cd} F_{cd}. \quad (1.56)$$

1.6 The Einstein Field Equation

Define the generic form of the Einstein-Hilbert action before starting to derive the field equation.

$$S = \int L\sqrt{-g} d^4x. \quad (1.57)$$

For a gravitational source and matter, the Lagrangian L is defined as $L = L_G + L_m$ where L_G is the Lagrangian for the gravitational field and L_m is the Lagrangian for matter.

$$S = \int \frac{1}{2\kappa} R\sqrt{-g} d^4x + \int L_m\sqrt{-g} d^4x. \quad (1.58)$$

where $\kappa = \frac{8\pi G}{c^4}$ and R is the Ricci scalar. Throughout this thesis, the speed of light c and the gravitational constant G are taken to be 1.

By least action principle, We take $\delta S = 0$, using this and equation (1.30) in (1.58) gives

$$\begin{aligned} \delta S &= \frac{1}{2\kappa} \int \left(R_{ab}g^{ab}\delta\sqrt{-g} + R_{ab}\sqrt{-g}\delta g^{ab} + \sqrt{-g}g^{ab}(\delta R_{ab}) \right) d^4x \\ &+ \int (L_M\delta\sqrt{-g} + \sqrt{-g}\delta(L_M)) d^4x = 0. \end{aligned} \quad (1.59)$$

Now consider coordinates at an arbitrary point P , where $\Gamma_{bc}^a = 0$. This then reduces the Riemann tensor to

$$R_{bcd}^a = \partial_c\Gamma_{bd}^a - \partial_d\Gamma_{bc}^a. \quad (1.60)$$

Applying δ on both sides of equation (1.60) yields

$$\delta R_{adb}^c = \delta\Gamma_{ab,d}^c - \delta\Gamma_{ad,b}^c. \quad (1.61)$$

Since the partial derivative commutes with variation and is equal to the covariant derivative in geodesic coordinates. The renowned Palatini equation is found to be

$$\delta R_{adb}^c = \delta\Gamma_{ab;d}^c - \delta\Gamma_{ad;b}^c. \quad (1.62)$$

Contraction of c and d gives

$$\delta R_{ab} = \delta\Gamma_{ab;c}^c - \delta\Gamma_{ac;b}^c, \quad (1.63)$$

multiplying above equation by g^{ab}

$$g^{ab}\delta R_{ab} = g^{ab}\delta\Gamma_{ab;c}^c - g^{ab}\delta\Gamma_{ac;b}^c, \quad (1.64)$$

$$= g^{ab}\delta\Gamma_{ab;c}^c - g^{ac}\delta\Gamma_{ab;c}^b, \quad (1.65)$$

$$= (g^{ab}\delta\Gamma_{ab}^c - g^{ac}\delta\Gamma_{ab}^b);_c. \quad (1.66)$$

Writing

$$A^c = g^{ab}\delta\Gamma_{ab}^c - g^{ac}\delta\Gamma_{ab}^b, \quad (1.67)$$

equation (1.66) becomes

$$g^{ab}\delta R_{ab} = A^c_{;c}. \quad (1.68)$$

Integrating equation (1.68) over the volume V , we have

$$\int_V g^{ab} \delta R_{ab} \sqrt{-g} d^4x = \int_V A_{;c}^c \sqrt{-g} d^4x, \quad (1.69)$$

using the divergence theorem, the left hand side of the equation (1.69) vanishes, i.e.

$$\int_V g^{ab} \delta R_{ab} \sqrt{-g} d^4x = 0. \quad (1.70)$$

By equation (1.70) and substitution of the identity $\delta\sqrt{-g} = -\frac{1}{2}\sqrt{-g}g^{ab}\delta g_{ab}$, equation (1.59) becomes:

$$\begin{aligned} & 2\kappa \int_V \left[R_{ab} g^{ab} \left(-\frac{1}{2} \sqrt{-g} g^{ab} \delta g_{ab} \right) + R_{ab} \sqrt{-g} \delta g^{ab} \right] d^4x \\ & + \int_V \left[L_m \left(-\frac{1}{2} \sqrt{-g} g^{ab} \delta g_{ab} \right) + \sqrt{-g} \delta(L_m) \right] d^4x = 0. \end{aligned} \quad (1.71)$$

As $L_m = L_m(g_{ab})$, this implies $\delta L_m = \frac{\partial L_m}{\partial g_{ab}} \delta g_{ab}$, thus equation (1.71) becomes:

$$\begin{aligned} & \frac{1}{2\kappa} \int_V \left(-\frac{1}{2} R g^{ab} \delta g_{ab} + R^{ab} \delta g_{ab} \right) \sqrt{-g} d^4x \\ & - \frac{1}{2} \int_V \left(-2 \frac{\partial L_m}{\partial g_{ab}} + L_m g^{ab} \right) \delta g_{ab} \sqrt{-g} d^4x = 0. \end{aligned} \quad (1.72)$$

Energy momentum tensor in terms of Lagrangian is defined as

$$T_{ab} = -2 \frac{\partial L_m}{\partial g_{ab}} + L_m g^{ab}. \quad (1.73)$$

Thus equation (1.72) takes the form

$$\frac{1}{2\kappa} \int_V \left(R_{ab} - \frac{1}{2} g_{ab} R - \kappa T_{ab} \right) \delta g^{ab} \sqrt{-g} d^4x = 0, \quad (1.74)$$

for arbitrary δg_{ab}

$$R_{ab} - \frac{1}{2} g_{ab} R = \kappa T_{ab}. \quad (1.75)$$

famous Einstein equation (1.75), on the left, indicates the existence of a gravitational source; on the right, an energy-momentum tensor indicates the location of matter in a particular place.

Chapter 2

Exact Solutions for Anisotropic Compact Stars in General Relativity

2.1 Exact Solutions

It is well known that the general theory of relativity is a non-linear theory from its very beginning. Because of this, it was and remained associated with severe difficulties when it came to achieving a profound understanding of the theory. Another important strategy used for dealing with this non-linearity as well as to gain a much more profound understanding of the phenomena has been the search for the exact solutions to the Einstein field equations. It could be worthwhile to highlight here that such solutions represent perhaps the most tractable ones that are also non-linear in their core according to the definitions given by Mason and Woodhouse [13]. This remarkable mathematical quality enables researchers to analyze and investigate non-linear functions and processes and compare them with systems that possess rather comprehensive and clear-cut solutions. These specific examples are important because, in practice, such exact solutions allow scientists to investigate the subtle non-linear features of GR while still retaining the manageable complexity that can be further examined and well understood by researchers who work in the field of the theory. Building practical exact solutions of the theory has proven to be a significant challenge even after a century of theoretical research, even though exact solutions do offer a great deal of information and applications useful in the study of GR. Because the Einstein field equations consist of up to 10 nonlinear partial differential equations, the process of deriving the solution is rather extensive. Because of this, in order to continue, a number of logical presumptions must be made, and all known precise solutions can only be reached by enforcing a set of conditions. Generally, metrics are subject to certain symmetry criteria to reduce complexity. Other circumstances like non-charged spacetimes, stationary, or static spacetimes might also be taken into account [15]. Consequently, to move toward a solution, it becomes necessary to make reasonable assumptions on the stress-energy tensor T_{ab} such as to consider its fluid forms like dust, perfect fluid or any form fit for an applicable category. However, this is possible if and only if all mathematical and physical assumptions made through the derivation of the solution yield a physically acceptable solution that will conform to the laws of GR in the background. Among them, one of the most established physical principles methods is to search for solutions by Equation of State, where it relates pressure in terms of energy density $p = p(\rho)$. By using this equation of state, the researchers are thus able to obtain

answers that are appropriate in describing the physical property character and behavior of the specific system in issue [16].

2.2 Compact Objects

Compact objects in GR are astrophysical objects defined by their great density and strong gravitational fields. The three kinds of compact objects are white dwarfs, neutron stars, and black holes. These objects represent the latter phases of star development and are of significant interest in astrophysics and GR owing to their unique features and the severe circumstances they produce.

2.2.1 White Dwarfs

The first known white dwarf, Sirius B, was found in 1844 by Friedrich Wilhelm Bessel, a German physicist who had seen a weak star marking Sirius' partner. Subrahmanyan Chandrasekhar, an Indian-American scientist, determined a basic upper limit to the mass that a non-rotating white dwarf may reach before becoming unstable in 1930. This limit, which is around 1.4 solar masses, is referred to as the Chandrasekhar limit. Beyond this threshold, a white dwarf will experience more gravitational collapse, which might result in the creation of a neutron star or a supernova explosion [18].

2.2.2 Neutron Stars

Supernova explosions occur when huge stars that have finished consuming their fuel exceed the Chandrasekhar limit. This explosion blows a star's outer layers apart, creating supernova debris. Neutron stars are created when protons and electrons in the center area collapse so that neutron degeneracy pressure partially prevents further collapse. Similar to how electron degeneracy pressure prevents white dwarfs from collapsing, neutron degeneracy pressure, a phenomenon explained by the Pauli exclusion principle, partially supports neutron stars from continuing to collapse. They were found to be radio pulsars at the close of the 1960s and X-ray stars at the beginning of the 1970s. One neutron star was found to host planets. Usually, their radius is around 10 km, and the highest mass of planets found in a single neutron star is predicted to be $3M_{\odot}$. This is because large stars are unable to withstand the force of gravity and eventually collapse [18]. *PSR J0740+6620* is the most massive neutron star has the mass about 2.1 solar mass.

2.2.3 Black Holes

Black holes, in particular, are compact objects that are the densest forms of objects in the cosmos. Because of the intense gravitational force from which even light is unable to escape, huge stars with core masses greater than three times that of the Sun may experience the complete collapse of their core into a black hole. The event horizon, which serves as a limit beyond which events cannot impact an outside observer, is a crucial component of black holes. It defines the boundary between those spacetime points that are still able to link to infinity via a timelike path and those that are not. Anything that passes over the event horizon will eventually approach the singularity of the black hole,

which is an incredibly dense and tiny point where standard physics breaks down. In order to avoid a black hole's hold, one would have to travel faster than light [16]. Compact objects, specifically black holes, represent the densest forms of matter in the universe. In massive stars with a core mass exceeding three times that of the Sun, the core may collapse into a black hole due to the overwhelming gravitational pull that not even light can escape. A key feature of black holes is the event horizon, which acts as a boundary beyond which events cannot affect an outside observer. It delineates the limit at which spacetime points can still connect to infinity through a timelike path from those that cannot. Once anything crosses the event horizon, it inevitably plunges toward the black hole's singularity, an infinitely small and dense point where conventional physics ceases to apply. To escape the grasp of a black hole, one would need to surpass the speed of light. For example, Sagittarius A^* is a black hole at the center of the Milky Way, which has about 4 million times the sun's mass.

2.3 Exploring Notable Exact Solutions of Einstein's Field Equations

Spacetime is described in GR as a four-dimensional pseudo-Riemannian manifold M . Since the corresponding metric is not positive definite, the signature may be expressed as $(-1, +1, +1, +1)$ or $(+1, -1, -1, -1)$. Equation (1.17) illustrates how the general line element is represented in terms of metric components. Unless otherwise indicated, the work done in this thesis is based on a static, spherically symmetric paraboloidal spacetime metric and is assumed to have a signature $(-1, +1, +1, +1)$. When considering solutions, particularly exact solutions, assuming symmetry is pivotal due to the mathematical simplifications it allows. Numerous successful theoretical predictions for spherically symmetric solutions have been made, validating Einstein's theory [17]. Therefore, by assuming spherical symmetry, the line element described in equation (1.16) and expressed in spherical coordinates will be transformed accordingly,

$$ds^2 = -c^2 dt^2 + dr^2 + r^2 d\Omega^2, \quad (2.1)$$

where $d\Omega^2 = d\theta^2 + \sin^2 \theta d\phi^2$. Now, for the metric to meet the requirement of being static, consider time independence. Static spacetime is defined as follows: "In a static spacetime, all metric components g_{ab} are independent of some timelike coordinate, say x^0 , and the line element is invariant under the transformation $x^0 \rightarrow -x^0$ " [11]. Next, if there is no preferable angular direction in space, the metric is spherically symmetric, i.e., $dx^a \rightarrow -dx^a$ where x^a are spatial coordinates. Thus, when $r \rightarrow \infty$ and in the presence of spherical symmetry, the metric in equation (2.1) becomes:

$$ds^2 = -e^{2\nu(r)} c^2 dt^2 + e^{2\lambda(r)} dr^2 + r^2 (d\theta^2 + \sin^2 \theta d\phi^2). \quad (2.2)$$

2.3.1 Schwarzschild Solution

In 1916, Schwarzschild introduced a fundamental exact solution by analyzing a vacuum scenario, transforming the Einstein field equation accordingly into

$$R_{ab} = 0. \quad (2.3)$$

For static and spherically symmetric metric provided in equation (2.2), the metric tensor and its inverse are as follows: The metric tensor g_{ab} and its inverse g^{ab} are given by:

$$g_{ab} = \begin{pmatrix} -e^{2\nu(r)} & 0 & 0 & 0 \\ 0 & e^{2\lambda(r)} & 0 & 0 \\ 0 & 0 & r^2 & 0 \\ 0 & 0 & 0 & r^2 \sin^2 \theta \end{pmatrix}, \quad g^{ab} = \begin{pmatrix} -e^{-2\nu(r)} & 0 & 0 & 0 \\ 0 & e^{-2\lambda(r)} & 0 & 0 \\ 0 & 0 & \frac{1}{r^2} & 0 \\ 0 & 0 & 0 & \frac{1}{r^2 \sin^2 \theta} \end{pmatrix}. \quad (2.4)$$

The total independent Christoffel symbols are 40, but the non-zero components are

$$\begin{aligned} \Gamma_{00}^1 &= \nu' e^{2(\nu-\lambda)}, & \Gamma_{22}^1 &= -r e^{2\lambda}, & \Gamma_{11}^1 &= \lambda', & \Gamma_{21}^2 &= \Gamma_{31}^3 = \frac{1}{r}, \\ \Gamma_{33}^1 &= -r e^{-2\lambda} \sin^2 \theta, & \Gamma_{33}^2 &= -\sin \theta \cos \theta, & \Gamma_{32}^3 &= \cot \theta, & \Gamma_{01}^0 &= \nu'. \end{aligned} \quad (2.5)$$

The non-vanishing components of the Ricci curvature tensor are

$$R_{00} = \nu'' + \nu'(\nu' - \lambda') + \frac{2\nu'}{r} = 0, \quad (2.6)$$

$$R_{11} = -\nu'' + \lambda'(\lambda' - \nu') + \frac{2\lambda'}{r} = 0, \quad (2.7)$$

$$R_{22} = 1 - e^{-2\lambda} + r e^{-2\lambda}(\lambda' - \nu') = 0, \quad (2.8)$$

$$R_{33} = R_{22} \sin^2 \theta = 0. \quad (2.9)$$

Simplifying equations (2.6) and (2.7) and further substituting it in equation (2.8) yields

$$\nu = -\lambda, \quad (2.10)$$

$$(r e^{-2\lambda})' = 1. \quad (2.11)$$

This implies

$$e^{2\nu} = e^{-2\lambda} = \left(1 + \frac{\alpha}{r}\right), \quad (2.12)$$

using weak field approximation, $\alpha = \frac{-2GM}{c^2}$ [11]. Thus the metric in equation (2.2) takes the form

$$ds^2 = - \left(1 - \frac{2GM}{c^2 r}\right) c^2 dt^2 + \left(1 - \frac{2GM}{c^2 r}\right)^{-1} dr^2 + r^2(d\theta^2 + \sin^2 \theta d\phi^2). \quad (2.13)$$

Where $m = \frac{GM}{c^2}$. The above metric for $G = c = 1$ becomes

$$ds^2 = - \left(1 - \frac{2m}{r}\right) dt^2 + \left(1 - \frac{2m}{r}\right)^{-1} dr^2 + r^2(d\theta^2 + \sin^2 \theta d\phi^2), \quad (2.14)$$

which is the Schwarzschild line element [19]. Event horizon of the Schwarzschild black hole is given by $r_s = \frac{2GM}{c^2}$. There exist two singularities in the metric (2.14). At $r = 0$ there is an essential singularity which cannot be removed, and at $r = 2m$ there is a coordinate singularity which can be removed by appropriate choice of coordinates.

2.3.2 Reissner-Nordstrom Solution

The analogous solution for a charged point mass was independently discovered by Reissner in 1916 [20] and by Nordström in 1918 [21], leading to what is now known as the Reissner-Nordström solution. Incorporating charge into the previous assumptions, the Einstein-Maxwell field equation becomes

$$R_{ab} = 8\pi T_{ab}. \quad (2.15)$$

In the case of spherical symmetry with a point charge placed at the origin, the components of the electrostatic field are in the radial direction, i.e., $E = E(r)$, with the magnetic field being zero. The Maxwell tensor F_{ab} in this case takes the form:

$$F_{ab} = \begin{pmatrix} 0 & -E(r) & 0 & 0 \\ E(r) & 0 & 0 & 0 \\ 0 & 0 & 0 & 0 \\ 0 & 0 & 0 & 0 \end{pmatrix} \quad (2.16)$$

It should satisfy the Maxwell equations. By plugging in the assumptions and using the metric and Christoffel symbols given in equations (2.4) and (2.5), we may write the Maxwell equation as $F_{;b}^{ab} = \frac{1}{\sqrt{-g}}\partial_b\sqrt{-g}F^{ab} = 0$. Because F^{ab} is not symmetric [11], the Maxwell equation reduces to:

$$\left(e^{-(\nu+\lambda)}\frac{E}{r^2}\right)' = 0. \quad (2.17)$$

By integrating, we get

$$E(r) = Qe^{(\nu+\lambda)}\frac{1}{r^2}, \quad (2.18)$$

Components of Maxwell energy-momentum tensor T_{ab} can be calculated from equation (1.56), i.e.

$$T_{ab} = (-E^2, -E^2, E^2, E^2). \quad (2.19)$$

Similarly, by using equation (2.19) in (2.15) together with the set of equations (2.6) to (2.8) and once again going through the comprehensive process, these equations then produce

$$\nu = -\lambda, \quad (2.20)$$

$$\left(re^{-2\lambda}\right)' = 1 - \frac{Q^2}{r^2}. \quad (2.21)$$

By integrating it we get,

$$e^{2\nu} = e^{-2\lambda} = \left(1 + \frac{\text{constant}}{r} + \frac{Q^2}{r^2}\right) \quad (2.22)$$

If $Q = 0$, then equation (2.22) reduces to Schwarzschild metric, which implies $Constant = -\frac{2GM}{c^2}$ and $m = \frac{GM}{c^2}$, thus the above equation becomes

$$e^{2\nu} = e^{-2\lambda} = \left(1 - \frac{2m}{r} + \frac{Q^2}{r^2}\right). \quad (2.23)$$

Hence, the Reissner-Nordstrom metric is

$$ds^2 = - \left(1 - \frac{2m}{r} + \frac{Q^2}{r^2}\right) dt^2 + \left(1 - \frac{2m}{r} + \frac{Q^2}{r^2}\right)^{-1} dr^2 + r^2 (d\theta^2 + \sin^2 \theta d\phi^2) \quad (2.24)$$

At $r = 0$, there is an essential singularity. To identify further singularities take,

$$1 - \frac{2m}{r} + \frac{Q^2}{r^2} = 0, \quad (2.25)$$

which implies,

$$r_{\pm} = m \pm \sqrt{m^2 - Q^2}. \quad (2.26)$$

On the surface, a coordinate singularity occurs at $r = r_{\pm}$, where r_+ is referred to as the outer horizon and r_- is referred to as the inner horizon. There exist three cases depending on the values of m and Q , which are as follows [11]:

1. If $m^2 < Q^2$: There is no coordinate singularity. This phenomenon is referred to as a naked singularity and is often regarded as lacking physical credibility.
2. If $m^2 > Q^2$: On surface $r = r_{\pm}$ two coordinate singularities occur. This situation is called a normal Reissner-Nordstrom black hole.
3. If $m^2 = Q^2$: This situation is termed a severe Reissner-Nordstrom black hole and is similar to the second instance but with the area $r_- < r < r_+$ deleted.

2.4 Admissible Conditions for Compact Objects

For any compact object to be considered physically suitable, it must satisfy the following conditions:

1. There must not be any singularity in the metric potentials within the object's radius.
2. Both the anisotropic factor and the electric field must be zero at the center and should increase as one approaches the boundary.
3. ρ , p_r , and p_t must be positive, decreasing monotonically with radial coordinates, and finite within the compact object.
4. The pressures p_r and p_t must be equal at the center of the compact object and at the boundary of the compact object p_r must be zero.
5. The trace of the energy-momentum tensor must be positive and decreasing.
6. The value of adiabatic index must be larger than $\frac{4}{3}$.
7. Energy, causality, and hydrostatic equilibrium conditions should be satisfied.

2.5 Review of Model of a Static Spherically Symmetric Anisotropic Fluid Distribution in Paraboloidal Spacetime Admitting a Polytropic Equation of State

S. Thirukkanesh, Ranjan Sharma and Shyam Das [25]

Introduction

In relativistic astrophysics, mathematical models of compact objects are crucial for comprehending the fundamental physical characteristics of these dense compact stars. Recently, the study of pressure anisotropy has become a significant focus in modeling compact stars, among other influencing factors. Herrera [40] has emphasized that anisotropic pressure within the interior of a relativistic compact star cannot be overlooked due to the various physical processes typically associated with such highly compact objects. To develop a model of a compact star, it is crucial to understand its composition, particularly in relation to a barotropic equation of state (EOS) of the form $p_r = p_r(\rho)$, which relates the radial pressure to the density of the matter distribution. For instance, 'strange stars' composed of quark matter are frequently modeled using a simple linear equation of state (EOS) in the MIT Bag model [41]. Several researchers have also employed a quadratic EOS to model compact stars [42]. Bhar et al. [43] developed an anisotropic stellar model filled with Chaplygin gas, while Ragel and Thirukkanesh [44] demonstrated that a Van der Waals type EOS could represent a relatively low-density star with a mixed fluid distribution. Stellar models using polytropic equations of state (EOS) have also been employed to represent compact objects with anisotropic fluid distributions.

The field equations in paraboloidal spacetime

If paraboloidal spacetime is embedded in a spherically symmetric static metric given by equation (2.2), initiating with the Cartesian equation of a Euclidean space characterizing as being four-dimensional with an immersed three paraboloid is given as

$$x^2 + y^2 + z^2 = 2wL, \quad (2.27)$$

here L is a constant, whereas a three-paraboloid is specified by the constants (x, y, z) and the constant w represents the sections of the sphere. The 3-paraboloid immersed in four-dimensional space is parameterized by using the following parameterizations earlier stated by Thomas and Pandya [27]:

$$x = r \sin \theta \cos \phi, \quad (2.28)$$

$$y = r \sin \theta \sin \phi, \quad (2.29)$$

$$z = r \cos \theta, \quad (2.30)$$

$$w = \frac{r^2}{2L}. \quad (2.31)$$

Thus by equation (2.28) to (2.31) the Euclidean metric

$$ds^2 = dx^2 + dy^2 + dz^2 + dw^2, \quad (2.32)$$

takes the form

$$ds^2 = \left(1 + \frac{r^2}{L^2}\right) dr^2 + r^2(d\theta^2 + \sin^2 \theta d\phi^2). \quad (2.33)$$

Here comparing equation (2.33) with equation (2.2) yields

$$e^{2\lambda} = 1 + \frac{r^2}{L^2}. \quad (2.34)$$

Thus, the interior stellar structure in a spherically symmetric, paraboloidal spacetime is given by the metric

$$ds^2 = -e^{2\nu} dt^2 + \left(1 + \frac{r^2}{L^2}\right) dr^2 + r^2(d\theta^2 + \sin^2\theta d\phi^2). \quad (2.35)$$

For anisotropic fluid distribution the components of energy momentum tensor T_{ab} are

$$T_{ab} = \text{diag}(-\rho, p_r, p_t, p_t). \quad (2.36)$$

So the field equations are given as

$$\frac{1}{r^2} \left(r \left(1 - e^{-2\lambda} \right) \right)' = \rho, \quad (2.37)$$

$$e^{-2\lambda} \frac{2}{r} \nu' - \frac{1}{r^2} \left(1 - e^{-2\lambda} \right) = p_r, \quad (2.38)$$

$$e^{-2\lambda} \left(\nu'' + \nu'^2 - \nu' \lambda' + \frac{1}{r} (\nu' - \lambda') \right) = p_t, \quad (2.39)$$

$$\frac{1}{2} \int_0^r w^2 (\rho(w)) dw = m(r). \quad (2.40)$$

2.5.1 Polytropic Models

Assuming the polytropic equation of state

$$p_r = k\rho^{1+1/\eta} - \beta, \quad (2.41)$$

along with the transformations

$$x = \frac{r^2}{L^2}, \quad (2.42)$$

$$y^2(x) = e^{2\nu(r)}, \quad (2.43)$$

$$z(x) = e^{-2\lambda(r)}, \quad (2.44)$$

where

$$z(x) = \frac{1}{1+x} \quad (2.45)$$

here k and β are constants. Thus, by these substitutions the system of equations are given as

$$\rho = \frac{1}{L^2} \left(1 - \frac{z}{x} - 2z' \right), \quad (2.46)$$

$$p_r = k\rho^{1+1/\eta} - \beta, \quad (2.47)$$

$$\Delta = \frac{1}{L^2} \left(4xz \frac{y''}{y} + z' \left(1 + 2x \frac{y'}{y} \right) + \frac{1-z}{x} \right), \quad (2.48)$$

$$\frac{y'}{y} = \frac{k}{4L^{2/\eta} z} \left(1 - \frac{z}{x} - 2z' \right)^{1+1/\eta} + \frac{1-z}{4xz} - \frac{\beta L^2}{4z}, \quad (2.49)$$

$$m(x) = \frac{L^3}{4} \int_0^x \sqrt{w(\rho(w))} dw. \quad (2.50)$$

Here ' represents derivative with respect to r .

2.5.2 Discussion

At boundary, $r = R$ authors have matched their solution to the Schwarzschild exterior spacetime i.e.

$$ds^2 = - \left(1 - \frac{2M}{r} \right) dt^2 + \left(1 - \frac{2M}{r} \right)^{-1} dr^2 + r^2 (d\theta^2 + \sin^2 \theta d\phi^2), \quad (2.51)$$

from which the total mass M and model parameter L are found as follows

$$M = m(R) = \frac{R^3}{2(L^2 + R^2)}, \quad (2.52)$$

$$L = \sqrt{\frac{R^3}{2M \left(1 - \frac{2M}{R} \right)}}. \quad (2.53)$$

Further, the boundary conditions imply the expression for the constant of integration and β in both cases as follows:

$$d_1^2 = \left(1 + \frac{R^2}{L^2} \right)^{-\left(1 + \frac{k}{2L^2} \right)} \times \exp \left[\frac{4k(3L^2 + 2R^2)}{(L^2 + R^2)^2} - \frac{R^2}{4L^2} (2 - \beta(2L^2 + R^2)) \right], \quad (2.54)$$

$$d_2^2 = \left(\frac{L^2}{L^2 + R^2} \right)^{(\sqrt{3L^2+R^2}-\sqrt{2L})/(\sqrt{3L^2+R^2}+\sqrt{2L})} \times \exp \left[-\frac{R^2}{4L^2} \left(\frac{4k\sqrt{3L^2+2R^2}}{(L^2+R^2)^2} + 2 - \beta(2L^2+R^2) \right) \right], \quad (2.55)$$

$$\beta_I = \frac{4kM^2(4M - 3R^2)}{R^8}, \quad (2.56)$$

$$\beta_{II} = \sqrt{\frac{8kM(3R - 4M)}{R^4}}. \quad (2.57)$$

Using the mass $M = 1.58M_\odot$ and radius $R = 9.1$ km of the pulsar 4U1820-30 in the above expressions, the conditions of acceptability are checked. The gravitational potentials are regular whereas density and pressures at the center ($r = 0$) yields $\rho(0) = \frac{3}{L^2}$ and

$p_r(0) = p_t(0) = \frac{9k}{L^2} - \beta$. The profiles are regular. Also, the metric functions are regular at the center.

Chapter 3

Charged Anisotropic Model with Chaplygin's Equation of State

3.1 Chaplygin's Equation of State

The Chaplygin gas model uses a particular form of the polytropic equation of state (EOS) given by the equation $p_r = \frac{A}{\rho^\alpha}$, where p represents pressure, ρ density, and A is a positive constant. In a generalised equation of state (EOS), the parameter α can take on values of either 1 or within the range $0 \leq \alpha \leq 1$. This particular equation of state (EOS) is beneficial for simulating unusual celestial bodies, including compact stars, that are capable of enduring highly demanding physical circumstances [45].

This chapter considers Chaplygin's equation of state in the presence of anisotropy and electromagnetic field on the backdrop of paraboloidal geometry, building on the work previously provided by Thirukkanesh et al.

The energy-momentum tensor for a charged anisotropic spherically symmetric compact object is obtained as

$$T_{ab} = T_{ab}^{matter} + T_{ab}^{EM}, \quad (3.1)$$

where

$$T_{ab}^{matter} = (\rho + p_r)u_a u_b + p_t g_{ab} + (p_r - p_t)n_a n_b, \\ T_{ab}^{EM} = \left(F_{a\alpha} F_b^\alpha - \frac{1}{4} g_{ab} F_{\alpha\beta} F^{\alpha\beta} \right).$$

Where $u_a = (1, 0, 0, 0)$ is the 4-velocity and n_a is the unit spacelike vector in the radial direction. By using the Maxwell energy-momentum tensor given in equation (2.19) and energy-momentum tensor for anisotropic matter distribution given in equation (2.36) we get

$$T_{ab} = \text{diag}(-\rho - E^2, p_r - E^2, p_t + E^2, p_t + E^2) \quad (3.2)$$

By taking into account the transformations provided by equation (2.42) – (2.44), where x , y , and z is the new independent coordinate and are new metric functions respectively, the modified version of the field equations (2.37)-(2.39) with energy-momentum tensor $T_{ab} = \text{diag}(\rho + E^2, p_r - E^2, p_t + E^2, p_t + E^2)$ is obtained.

$$\frac{1-z}{x} - 2\dot{z} = L^2(\rho + E^2) \quad (3.3)$$

$$\frac{4z\dot{y}}{y} - \frac{1-z}{x} = L^2(p_r - E^2) \quad (3.4)$$

$$4xz\dot{y} + (4z + 2x\dot{z})\frac{\dot{y}}{y} + \dot{z} = L^2(p_t + E^2) \quad (3.5)$$

$$\sigma^2 = \frac{4z}{xL^2}(x\dot{E} + E)^2 \quad (3.6)$$

where “.” represents derivative w.r.t x . The following is the mass function on the sphere's interior region with radius r :

$$M(r) = \frac{1}{2} \int_0^r \tilde{r}^2 dr \quad (3.7)$$

By using transformation (2.76), mass is transformed to

$$M(x) = \frac{L^3}{4} \int_0^x \sqrt{\tilde{x}} d\tilde{x} \quad (3.8)$$

3.2 Exact Solutions with Chaplygin's Equation of State

The Chaplygin's equation of state is given as [45]

$$p_r = \alpha\rho - \frac{\beta}{\rho}, \quad (3.9)$$

where as α, β are arbitrary constants. Using Chaplygin's equation of state and energy density given by equations (3.9) and (3.3) respectively in equation (3.2), we get the expression,

$$-\frac{4z}{L^2}\frac{\dot{y}}{y} + \frac{1-z}{xL^2} + \alpha\left(\frac{1-z}{xL^2} - \frac{2\dot{z}}{L^2} - E^2\right) - \frac{\beta}{\left(\frac{1-z}{xL^2} - \frac{2\dot{z}}{L^2} - E^2\right)} = 0 \quad (3.10)$$

Equation (3.10) implies,

$$\frac{\dot{y}}{y} = \frac{L^2(1+\alpha)}{4z}\left(\frac{1-z}{xL^2} - E^2\right) - \frac{L^2\beta}{4z\left(\frac{1-z}{xL^2} - \frac{2\dot{z}}{L^2} - E^2\right)} - \frac{\alpha\dot{z}}{2z} \quad (3.11)$$

To get an exact solution, using the ansatz E ,

$$E^2 = \frac{2\zeta ax}{1+x} \quad (3.12)$$

where ζ and a are arbitrary real constants. By putting the values of z given by equation (2.45) and E in (3.12), we get,

$$\frac{\dot{y}}{y} = \frac{L^2(1+\alpha)}{4}\left(\frac{1}{L^2} - 2\zeta ax\right) - \frac{L^2\beta(1+x)^2}{4\left(\frac{1}{L^2} + \frac{2}{L^2(1+x)} - 2\zeta ax\right)} + \frac{\alpha}{2(1+x)} \quad (3.13)$$

Equations (3.3) and (3.6) provide the energy density and charge density expressions, which will take the form,

$$\rho = \frac{3 + x - 2\zeta axL^2(1 + x)}{L^2(1 + x)^2} \quad (3.14)$$

$$\sigma^2 = \frac{2a\zeta(3 + 2x)^2}{L^2(1 + x)^4} \quad (3.15)$$

3.2.1 Chaplygin's Model

Here, the exact solution to Einstein's field equations in the presence of anisotropy and the electromagnetic field is presented. The radial and azimuth pressures for the current model, which uses z and E , has the following form,

$$p_r = \alpha \left(\frac{3 + x - 2\zeta axL^2(1 + x)}{L^2(1 + x)^2} \right) - \frac{\beta(L^2(1 + x)^2)}{(3 + x - 2\zeta axL^2(1 + x))} \quad (3.16)$$

$$\begin{aligned} p_t = & -\frac{2a\zeta x}{x+1} + \frac{-\frac{1}{(x+1)^2}}{L^2} + \frac{\left(\frac{4}{x+1} - \frac{2x}{(x+1)^2}\right) \left(\frac{1}{4}(\alpha+1)L^2\left(\frac{1}{L^2} - 2a\zeta x\right) + \frac{\alpha}{2(x+1)}\right)}{L^2} \\ & - \frac{\left(\frac{4}{x+1} - \frac{2x}{(x+1)^2}\right) \frac{\beta L^2(x+1)^2}{4\left(-2a\zeta x + \frac{2}{L^2(x+1)} + \frac{1}{L^2}\right)}}{L^2} \\ & + \frac{4x \left(-\frac{1}{2}a(\alpha+1)\zeta L^2 - \frac{\beta L^2(x+1)}{2\left(-2a\zeta x + \frac{2}{L^2(x+1)} + \frac{1}{L^2}\right)} + \frac{\beta L^2(x+1)^2 \left(-2a\zeta - \frac{2}{L^2(x+1)^2}\right)}{4\left(-2a\zeta x + \frac{2}{L^2(x+1)} + \frac{1}{L^2}\right)^2} - \frac{\alpha}{2(x+1)^2} \right)}{L^2(1+x)} \\ & + \frac{4x \left(\frac{1}{4}(\alpha+1)L^2\left(\frac{1}{L^2} - 2a\zeta x\right) - \frac{\beta L^2(x+1)^2}{4\left(-2a\zeta x + \frac{2}{L^2(x+1)} + \frac{1}{L^2}\right)} + \frac{\alpha}{2(x+1)} \right)^2}{L^2(1+x)} \end{aligned} \quad (3.17)$$

By integrating equation (3.13) we will get the gravitational potential y

$$y = K(x+1)^{\alpha/2} \times e^{U(x)} \times W(x)^m \quad (3.18)$$

Here K is constant of integration $U(x)$, $W(x)$, and m is

$$\begin{aligned} U(x) = & \frac{1}{4} \left(-a\alpha\zeta L^2 x^2 - a\zeta L^2 x^2 + \frac{\beta L^2(x+1)^2}{4a\zeta} + \alpha x + x + \frac{\beta(x+1)(2a\zeta L^2 + 1)}{4a^2\zeta^2} \right. \\ & \left. + \frac{\beta(2a\zeta L^2 + 1)(4a^2\zeta^2 L^4 + 16a\zeta L^2 + 1) \tan^{-1} \left(\frac{-2a\zeta L^2 + 4a\zeta L^2(x+1) - 1}{\sqrt{-4a^2\zeta^2 L^4 - 20a\zeta L^2 - 1}} \right)}{8a^3\zeta^3 L^2 \sqrt{-4a^2\zeta^2 L^4 - 20a\zeta L^2 - 1}} \right) \end{aligned}$$

$$W(x) = -2a\zeta L^2(x+1)^2 + 2a\zeta L^2(x+1) + x + 3$$

$$m = \frac{\beta(4a^2\zeta^2 L^4 + 8a\zeta L^2 + 1)}{64a^3\zeta^3 L^2}$$

The line element is determined by the gravitational potential y and $e^{2\lambda}$, which are represented by equations (3.20) and (2.68), respectively.

$$ds^2 = -K^2 \left(1 + \frac{r^2}{L^2}\right)^\alpha \exp \left[2U \left(\frac{r^2}{L^2}\right)\right] W \left(\frac{r^2}{L^2}\right)^{2m} dt^2 + \left(1 + \frac{r^2}{L^2}\right) dr^2 + r^2 \left(d\theta^2 + \sin^2 \theta d\phi^2\right) \quad (3.19)$$

3.2.2 Boundary Conditions

The Reissner-Nordstrom metric describes the exterior structure of a spherically symmetric, charged anisotropic spacetime. Which is

$$ds^2 = - \left(1 - \frac{2M}{r} + \frac{Q^2}{r^2}\right) dt^2 + \left(1 - \frac{2M}{r} + \frac{Q^2}{r^2}\right)^{-1} dr^2 + r^2(d\theta^2 + \sin^2 \theta d\phi^2) \quad (3.20)$$

At the boundary $r = R$, our solution must coincide with the Reissner-Nordstrom solution, which required

$$e^{2\nu} = -K^2 \left(1 + \frac{r^2}{L^2}\right)^\alpha \exp \left[2U \left(\frac{r^2}{L^2}\right)\right] W \left(\frac{r^2}{L^2}\right)^{2m} = \left(1 - \frac{2M}{R} + \frac{Q^2}{R^2}\right), \quad (3.21)$$

$$e^{-2\lambda} = \left(1 + \frac{r^2}{L^2}\right)^{-1} = \left(1 - \frac{2M}{R} + \frac{Q^2}{R^2}\right). \quad (3.22)$$

where M and Q are the total mass and charge respectively. The total mass at the boundary is determined by equation (3.22), is

$$M = \frac{R^3 + 2\xi a R^5}{2(L^2 + R^2)}. \quad (3.23)$$

By equation (3.23) we will get L ,

$$L = \left(\frac{R^3}{2M} (1 - 2a\xi R^2) - \frac{2M}{R}\right)^{1/2}. \quad (3.24)$$

By implying the boundary condition (3.21), we can get the constant of integration for our model.

$$K^2 = \left(\frac{L^2}{L^2 + R^2}\right)^{1+\alpha} \exp \left[-2U \left(\frac{r^2}{L^2}\right)\right] W \left(\frac{r^2}{L^2}\right)^{-2m} \quad (3.25)$$

The radial pressure must disappear at the star's boundary, i.e. $p_r(r = R) = 0$, By using this condition, we get

$$\beta = \alpha \left(\frac{-2a\zeta r^2 \left(\frac{r^2}{L^2} + 1\right) + \frac{r^2}{L^2} + 3}{L^2 \left(\frac{r^2}{L^2} + 1\right)^2}\right)^2 \quad (3.26)$$

Assumed Values Of Constant For Physical Analysis

To meet the criteria for physical analysis and stability condition, we have assumed the values of constant, which are, $L = 1.8$, $a = 1.089775$, $\zeta = 0.01$, and $\alpha = 0.06184373$ for the boundary r from 0 to 1. The value of β and constant of integration K is computed from the equations (3.26) and (3.25) respectively.

Constant	Values
K	$1.4181462075724175 \times 10^{-135}$
β	0.0216123301595

Table 3.1. Constant K and β

3.2.3 Physical Conditions

Metric Potentials

The most basic and most crucial requirement is to check the regularity of the metric potentials. The metric potential $e^{2\lambda}$ is 1 At the center and $e^{2\nu}$ is some positive constant. Figure 3.1 shows that bot metric potentials are singularity-free and monotonically increasing.

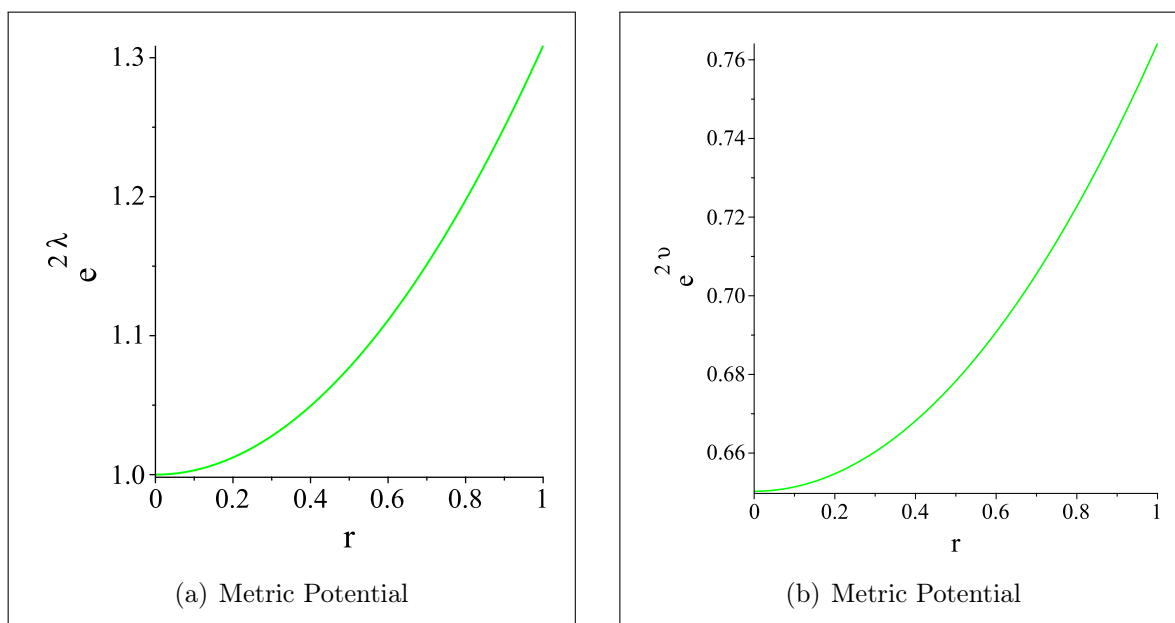


Figure 3.1: Graph of Metric Potentials are plotted for the constants: $L = 1.8$, $a = 1.08977$, $\zeta = 0.01$, and $\alpha = 0.06184373$ with respect to r .

Electric Field Intensity And Energy Density

Figure 3.2 illustrates the behavior of the electric field intensity, which is zero at the origin and increases as it approaches the star's boundary. This is because of the charge distribution at the surface of the star. The expression of density given in equation (3.14) by putting $x = \frac{r^2}{L^2}$ at the center is attained as

$$\rho_c = \frac{3}{L^2} > 0 \quad (3.27)$$

Accordingly, it can be inferred that energy density is not subject to central singularity, and Figure (3.3) illustrates how the density is decreasing.

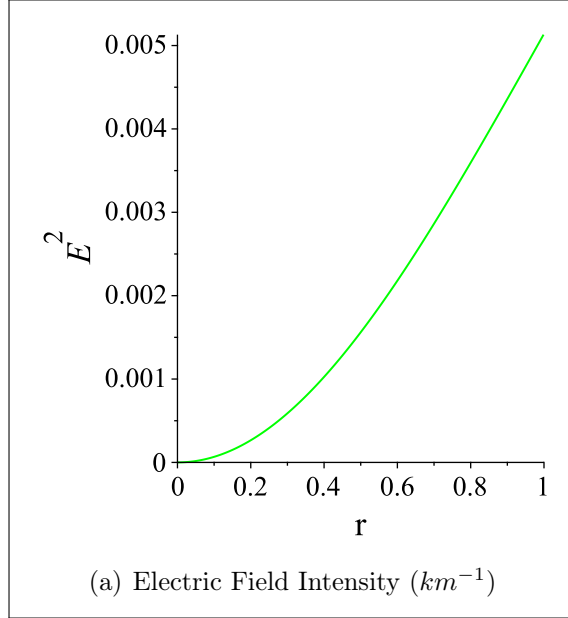


Figure 3.2: Graph of Electric Field Intensity is plotted for the constants: $L = 1.8$, $a = 1.08977$, $\zeta = 0.01$, and $\alpha = 0.06184373$ with respect to r .

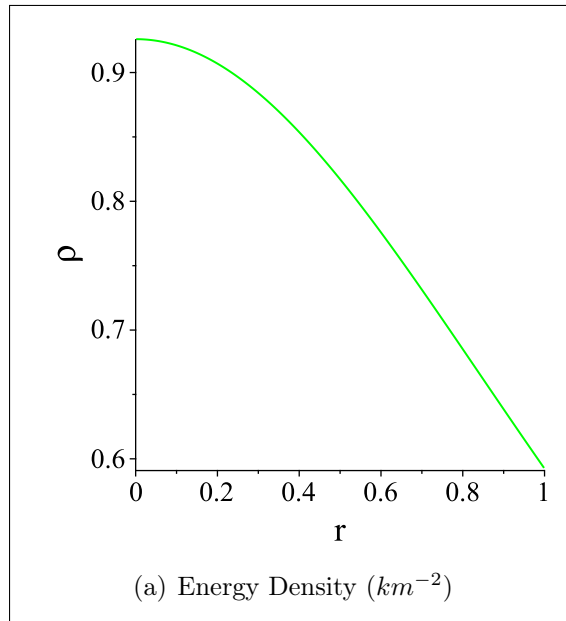


Figure 3.3: Graph of Energy Density is plotted for the constants: $L = 1.8$, $a = 1.08977$, $\zeta = 0.01$, and $\alpha = 0.06184373$ with respect to r .

Pressures

The radial and tangential pressure at the center can be determined by evaluating the corresponding expressions given in equation (3.16) and (3.17) respectively by putting $x = \frac{r^2}{L^2}$,

$$p_r(r = 0) = p_t(r = 0) = \frac{3\alpha}{L^2} - \frac{L^2\beta}{3} > 0. \quad (3.28)$$

This shows that both pressures are the same at the center and free from the central singularity. In Figure (3.4), we can see the decreasing behavior of radial pressure and it vanishes at the boundary. This is because the gravitational force at the center requires higher pressure to maintain the equilibrium. Tangential pressure also shows a decreasing nature as we move towards the boundary. For tangential pressure it is not necessary to be zero at the boundary.

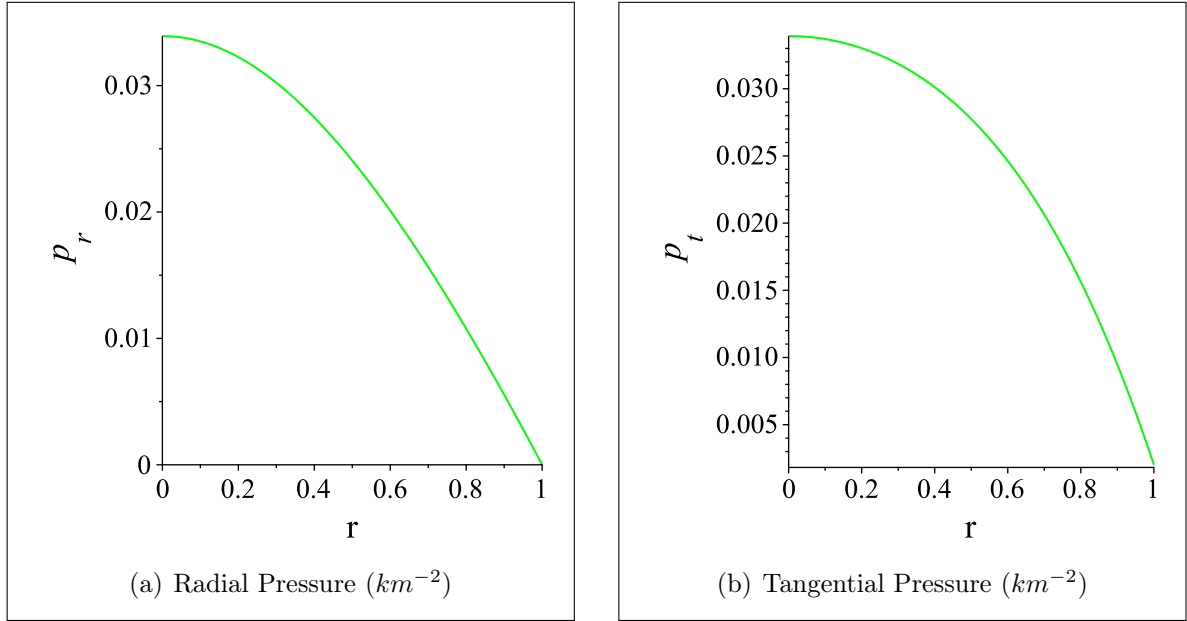


Figure 3.4: Graph of Pressures are plotted for the constants: $L = 1.8$, $a = 1.08977$, $\zeta = 0.01$, and $\alpha = 0.06184373$ with respect to r .

Pressures Density Ratios

To confirm the consistency of any physical solution, it is necessary to satisfy Zeldovich's requirements [28]. This means that the pressure density ratios in the center of the object must be less than 1, continuous, and positive throughout the core of the star, represented

by the equation $\left(\frac{p_r}{\rho}, \frac{p_t}{\rho}\right) \Big|_{r=0} \leq 1$. Hence,

$$\alpha - \frac{\beta L^4}{9} \leq 1 \quad (3.29)$$

Both pressure-density ratios decrease as r increases towards the surface. This is to be expected since gravitational forces in stars usually cause pressure to drop with increasing radius.

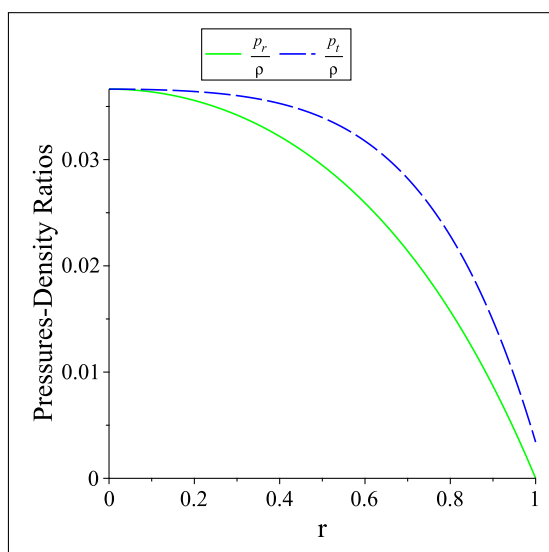


Figure 3.5: Graph of Pressure-Density Ratios are plotted for the constants: $L = 1.8$, $a = 1.08977$, $\zeta = 0.01$, and $\alpha = 0.06184373$ with respect to r . The green curve represents the ratio of radial pressure to energy density and the blue dashed curve represents the ratio of tangential pressure to energy density.

Trace of Energy Tensor

The energy tensor trace for our compact star model is graphed against the radial distance, r , in Figure 3.6. It is consistently positive and meets the criteria established by Bondi [29] for an anisotropic fluid sphere, which states that $\rho - p_r - 2p_t > 0$. Understanding how various pressures and densities affect the stability and structure of the star depends on this relationship. For example, if the pressure exceeds the energy density, it indicates a potential risk of collapse or other instabilities in the star.

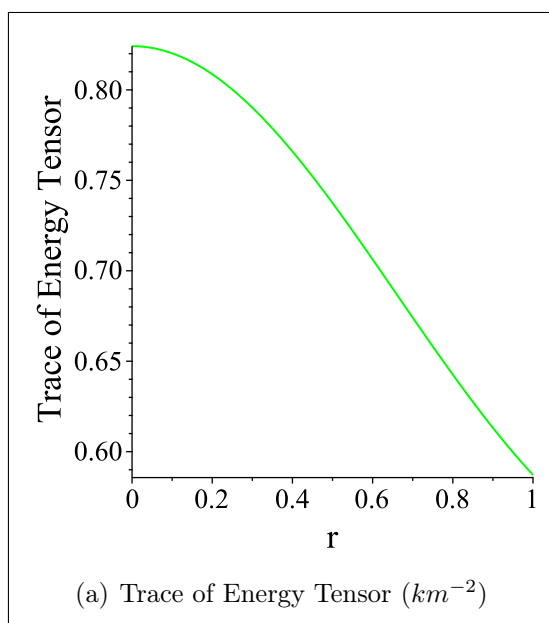


Figure 3.6: Graph of Energy Tensor Trace is plotted for the constants: $L = 1.8$, $a = 1.08977$, $\zeta = 0.01$, and $\alpha = 0.06184373$ with respect to r .

Anisotropic Factor

Anisotropy is defined as the difference between tangential and radial pressure. For the compact object, the anisotropic factor must be 0 at the core, as radial and tangential pressures are the same at the center and positive elsewhere, which is shown in Figure (3.7). It is highest at some intermediate regions where the forces are in balance and decreases towards the boundary where pressures decrease as well.

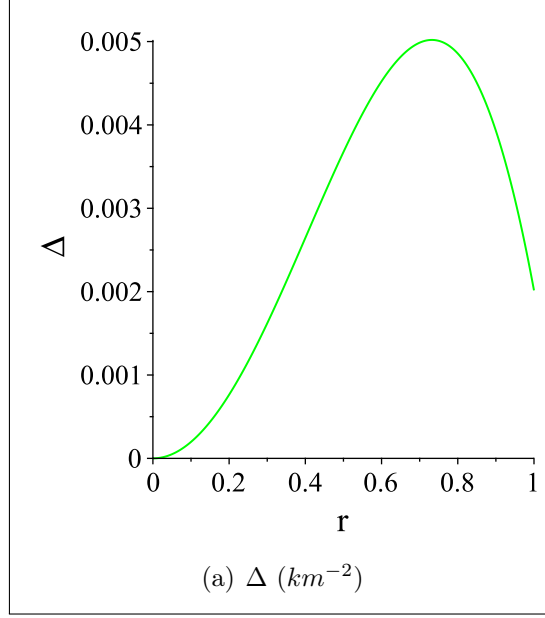


Figure 3.7: Graph of Anisotropic Factor is plotted for the constants: $L = 1.8$, $a = 1.08977$, $\zeta = 0.01$, and $\alpha = 0.06184373$ with respect to r .

Gradients

The following are the generalized formulations for our model's pressure and density gradients in the radial and transverse directions.

$$\frac{d\rho}{dr} = \frac{-\frac{4a\zeta r^3}{L^4} - \frac{4a\zeta r\left(\frac{r^2}{L^2} + 1\right)}{L^2} + \frac{2r}{L^2}}{L^2 \left(\frac{r^2}{L^2} + 1\right)^2} - \frac{4r \left(-\frac{2a\zeta r^2\left(\frac{r^2}{L^2} + 1\right)}{L^2} + \frac{r^2}{L^2} + 3 \right)}{L^4 \left(\frac{r^2}{L^2} + 1\right)^3} \quad (3.30)$$

$$\begin{aligned} \frac{dp_r}{dr} = & -\frac{4\beta r \left(\frac{r^2}{L^2} + 1\right)}{-\frac{2a\zeta r^2\left(\frac{r^2}{L^2} + 1\right)}{L^2} + \frac{r^2}{L^2} + 3} - \frac{4\alpha r \left(-\frac{2a\zeta r^2\left(\frac{r^2}{L^2} + 1\right)}{L^2} + \frac{r^2}{L^2} + 3 \right)}{L^4 \left(\frac{r^2}{L^2} + 1\right)^3} + \\ & \frac{\alpha \left(-\frac{4a\zeta r^3}{L^4} - \frac{4a\zeta r\left(\frac{r^2}{L^2} + 1\right)}{L^2} + \frac{2r}{L^2} \right)}{L^2 \left(\frac{r^2}{L^2} + 1\right)^2} + \frac{\beta L^2 \left(\frac{r^2}{L^2} + 1\right)^2 \left(-\frac{4a\zeta r^3}{L^4} - \frac{4a\zeta r\left(\frac{r^2}{L^2} + 1\right)}{L^2} + \frac{2r}{L^2} \right)}{\left(-\frac{2a\zeta r^2\left(\frac{r^2}{L^2} + 1\right)}{L^2} + \frac{r^2}{L^2} + 3 \right)^2} \end{aligned} \quad (3.31)$$

$$\begin{aligned}
\frac{dp_t}{dr} = & \frac{1}{2}r \left[\frac{8L^2}{(L^2+r^2)^3} + \frac{36L^2r^2\alpha}{(L^2+r^2)^4} - \frac{28L^2\alpha}{(L^2+r^2)^3} + \frac{8ar^2\zeta}{(L^2+r^2)^2} \right. \\
& - \frac{8a\zeta}{(L^2+r^2)} + \frac{12ar^2(1+\alpha)\zeta}{(L^2+r^2)^2} - \frac{16a(1+\alpha)\zeta}{(L^2+r^2)} \\
& - \frac{4r^2(1+\alpha)(-1+2ar^2\zeta)}{(L^2+r^2)^3} + \frac{6(1+\alpha)(-1+2ar^2\zeta)}{(L^2+r^2)^2} \\
& - \frac{16ar^2(L^2+r^2)^2\beta\zeta}{(L^2(-3+2ar^2\zeta)+r^2(-1+2ar^2\zeta))^2} + \frac{10(L^2+r^2)\beta}{L^2(-3+2ar^2\zeta)+r^2(-1+2ar^2\zeta)} \\
& - \frac{8r^2\beta\left(1+\frac{a(L^2+r^2)^2\zeta}{L^2}\right)}{(L^2(-3+2ar^2\zeta)+r^2(-1+2ar^2\zeta))^2} - \frac{8\left(1+\frac{r^2}{L^2}\right)\beta\left(1+\frac{a(L^2+r^2)^2\zeta}{L^2}\right)}{(-3+2ar^2\zeta+\frac{r^2(-1+2ar^2\zeta)}{L^2})^2} \\
& + \frac{16r^2(L^2+r^2)\beta(-1+2a(L^2+2r^2)\zeta)(aL^4\zeta+ar^4\zeta+L^2(1+2ar^2\zeta))}{(L^2(-3+2ar^2\zeta)+r^2(-1+2ar^2\zeta))^3} \\
& - \frac{12r^2\beta(aL^4\zeta+ar^4\zeta+L^2(1+2ar^2\zeta))}{(L^2(-3+2ar^2\zeta)+r^2(-1+2ar^2\zeta))^2} - \frac{8(L^2+r^2)\beta(aL^4\zeta+ar^4\zeta+L^2(1+2ar^2\zeta))}{(L^2(-3+2ar^2\zeta)+r^2(-1+2ar^2\zeta))^2} \\
& + \frac{2r^2\left(-\frac{2L^2\alpha}{(L^2+r^2)^2}-2a(1+\alpha)\zeta-\frac{(L^2+r^2)^3\beta(-1+2a(L^2+2r^2)\zeta)}{(L^2(-3+2ar^2\zeta)+r^2(-1+2ar^2\zeta))^2}+\frac{3(L^2+r^2)^2\beta}{L^2(-3+2ar^2\zeta)+r^2(-1+2ar^2\zeta)}\right)}{L^4\left(1+\frac{r^2}{L^2}\right)} \\
& - \frac{r^2\left(\frac{2L^2\alpha}{L^2+r^2}-(1+\alpha)(-1+2ar^2\zeta)+\frac{(L^2+r^2)^3\beta}{L^2(-3+2ar^2\zeta)+r^2(-1+2ar^2\zeta)}\right)^2}{L^6\left(1+\frac{r^2}{L^2}\right)^2} \\
& \left. + \frac{\left(\frac{2L^2\alpha}{L^2+r^2}-(1+\alpha)(-1+2ar^2\zeta)+\frac{(L^2+r^2)^3\beta}{L^2(-3+2ar^2\zeta)+r^2(-1+2ar^2\zeta)}\right)^2}{L^4\left(1+\frac{r^2}{L^2}\right)} \right] \tag{3.32}
\end{aligned}$$

The pressures and density gradients are graphed, and all of them have negative values as shown in Figures (3.8), (3.9) and (3.10). Within a stable star, the gravitational force pulling matter inward is balanced by the pressure gradient, which typically decreases outward from the core to the surface.

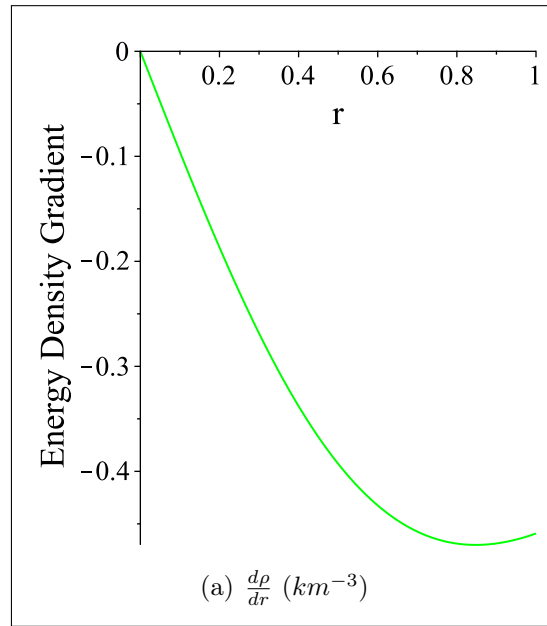


Figure 3.8: Graph of Density Gradient is plotted for the constants: $L = 1.8$, $a = 1.08977$, $\zeta = 0.01$, and $\alpha = 0.06184373$ with respect to r .

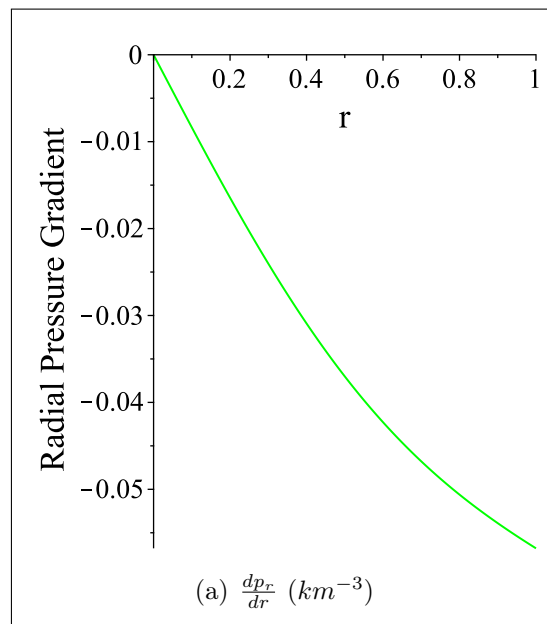


Figure 3.9: Graph of Radial Pressure Gradient is plotted for the constants: $L = 1.8$, $a = 1.08977$, $\zeta = 0.01$, and $\alpha = 0.06184373$ with respect to r .

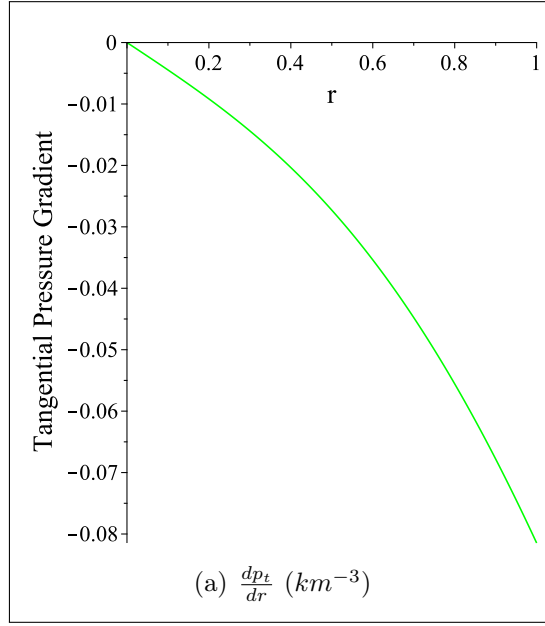


Figure 3.10: Graph of Tangential Pressure Gradient is plotted for the constants: $L = 1.8$, $a = 1.08977$, $\zeta = 0.01$, and $\alpha = 0.06184373$ with respect to r .

Mass and Compactness factor

We previously derived the mass function in equation (3.23). Buchdal [30] postulated that the ratio of mass to radius within a compact star should be smaller than $4/9$. In our current model, the ratio of mass to radius is $M/R = 0.120495$, which is less than $4/9$ as demonstrated in Figure (3.11) demonstrates the shape of the mass function, which is positive and smooth within the star's interior and zero at the center. The compactness factor for the compact star is expressed as follows:

$$\mu = \frac{M(r)}{r}. \quad (3.33)$$

The profile for our case is shown in Figure (3.12) which is increasing monotonically and is less than $4/9$. It classifies the compact object as follows [31]:

- Normal stars: $\frac{M}{r} \sim 10^{-5}$
- White dwarfs: $\frac{M}{r} \sim 10^{-3}$
- Neutron star: $10^{-1} < \frac{M}{r} < 0.25$
- Ultra-compact star: $0.25 < \frac{M}{r} < 0.5$
- Black hole: $\frac{M}{r} = 0.5$

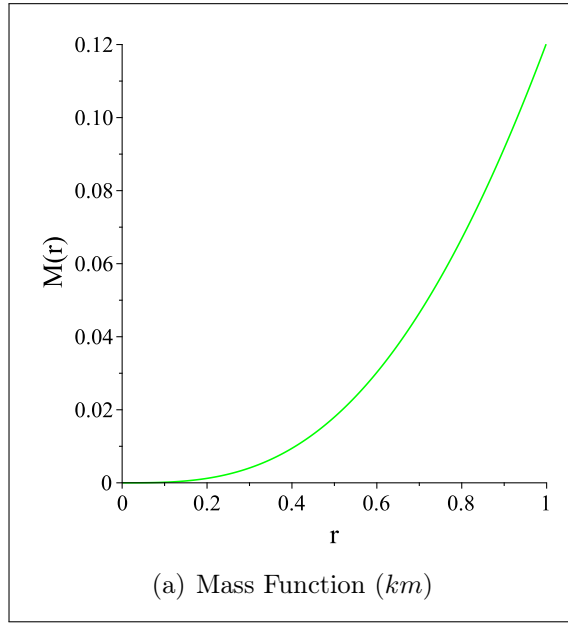


Figure 3.11: Graph of Mass is plotted for the constants: $L = 1.8$, $a = 1.08977$, $\zeta = 0.01$, and $\alpha = 0.06184373$ with respect to r .

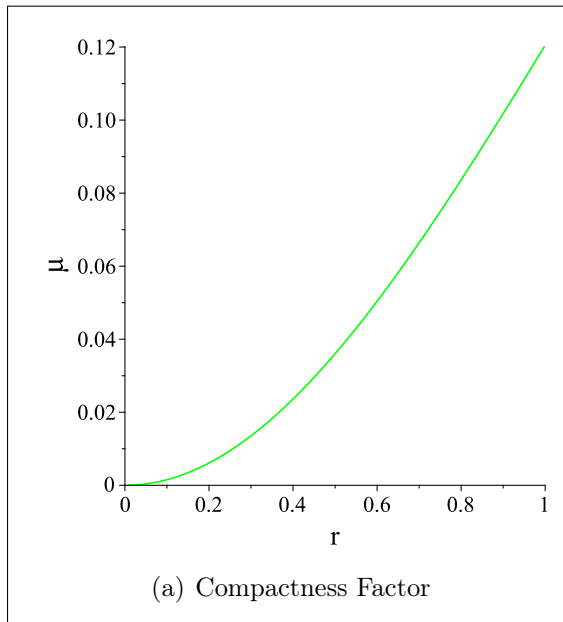


Figure 3.12: Graph of compactness Factor is plotted for the constants: $L = 1.8$, $a = 1.08977$, $\zeta = 0.01$, and $\alpha = 0.06184373$ with respect to r .

RedShifts

The expression of surface and gravitational redshifts are given as

$$z_s = e^\lambda - 1 = \left(1 + \frac{R^2}{L^2}\right)^{1/2} - 1 \quad (3.34)$$

$$z = e^{-\nu} - 1 \quad (3.35)$$

In this case, the surface redshift z_s is below 1, which is necessary for the model to be considered physically acceptable. This is shown in Figure (3.13a). It is zero at the center

and it is increasing monotonically as radius is increasing. This is because light needs to escape the gravitational field which results in a greater redshift for the light emitted from the surface compared to that emitted from the center. Moreover, gravitational redshift z as seen in Figure (3.13)*b* has a decreasing nature as per need.

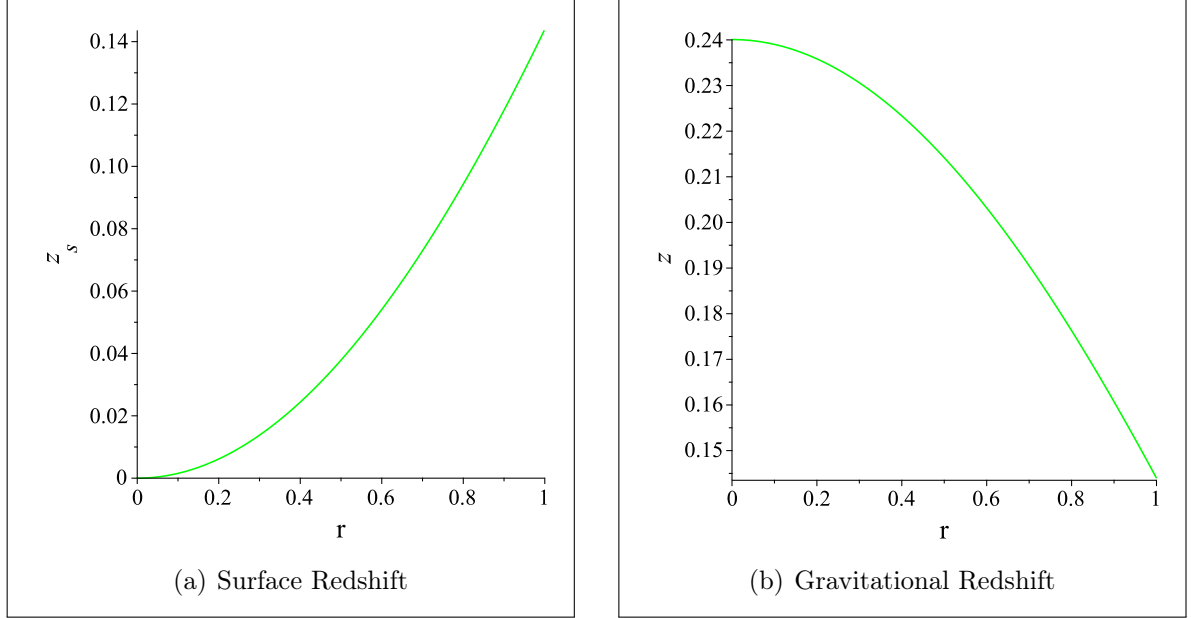


Figure 3.13: Graph of Surface and Gravitational Redshifts are plotted for the constants: $L = 1.8$, $a = 1.08977$, $\zeta = 0.01$, and $\alpha = 0.06184373$ with respect to r .

3.2.4 Stability Conditions

Casuality Condition

The speeds of sound in the radial and tangential directions for a distribution of anisotropic fluid are determined as

$$v_r^2 = \frac{dp_r}{d\rho} = \frac{\frac{dp_r}{dr}}{\frac{d\rho}{dr}} \quad (3.36)$$

$$v_t^2 = \frac{dp_t}{d\rho} = \frac{\frac{dp_t}{dr}}{\frac{d\rho}{dr}} \quad (3.37)$$

where in our circumstances the value of radial and tangential speeds of sound takes the form

$$\frac{dp_r}{d\rho} = \frac{1}{(L^2 r^2 (1 - 2a\zeta) - 2a\zeta r^4 + 3L^4)^2} \left(\begin{aligned} &\beta L^{12} + 4\beta L^{10} r^2 + L^8 (9\alpha + 6\beta r^4) \\ &+ 4a^2 \alpha \zeta^2 r^8 + 4a\alpha \zeta L^2 r^6 (2a\zeta - 1) \\ &+ L^4 r^4 (4a^2 \alpha \zeta^2 - 16a\alpha \zeta + \alpha + \beta r^4) \\ &+ 2L^6 (\alpha r^2 (3 - 6a\zeta) + 2\beta r^6) \end{aligned} \right) \quad (3.38)$$

$$\begin{aligned}
\frac{dp_t}{d\rho} = & \frac{1}{2}r \left[\frac{8L^2}{(L^2+r^2)^3} + \frac{36L^2r^2\alpha}{(L^2+r^2)^4} - \frac{28L^2\alpha}{(L^2+r^2)^3} + \frac{8ar^2\zeta}{(L^2+r^2)^2} \right. \\
& - \frac{8a\zeta}{(L^2+r^2)} + \frac{12ar^2(1+\alpha)\zeta}{(L^2+r^2)^2} - \frac{16a(1+\alpha)\zeta}{(L^2+r^2)} \\
& - \frac{4r^2(1+\alpha)(-1+2ar^2\zeta)}{(L^2+r^2)^3} + \frac{6(1+\alpha)(-1+2ar^2\zeta)}{(L^2+r^2)^2} \\
& - \frac{16ar^2(L^2+r^2)^2\beta\zeta}{(L^2(-3+2ar^2\zeta)+r^2(-1+2ar^2\zeta))^2} + \frac{10(L^2+r^2)\beta}{L^2(-3+2ar^2\zeta)+r^2(-1+2ar^2\zeta)} \\
& - \frac{8r^2\beta\left(1+\frac{a(L^2+r^2)^2\zeta}{L^2}\right)}{(L^2(-3+2ar^2\zeta)+r^2(-1+2ar^2\zeta))^2} - \frac{8\left(1+\frac{r^2}{L^2}\right)\beta\left(1+\frac{a(L^2+r^2)^2\zeta}{L^2}\right)}{\left(-3+2ar^2\zeta+\frac{r^2(-1+2ar^2\zeta)}{L^2}\right)^2} \\
& + \frac{16r^2(L^2+r^2)\beta(-1+2a(L^2+2r^2)\zeta)(aL^4\zeta+ar^4\zeta+L^2(1+2ar^2\zeta))}{(L^2(-3+2ar^2\zeta)+r^2(-1+2ar^2\zeta))^3} \\
& - \frac{12r^2\beta(aL^4\zeta+ar^4\zeta+L^2(1+2ar^2\zeta))}{(L^2(-3+2ar^2\zeta)+r^2(-1+2ar^2\zeta))^2} \\
& - \frac{8(L^2+r^2)\beta(aL^4\zeta+ar^4\zeta+L^2(1+2ar^2\zeta))}{(L^2(-3+2ar^2\zeta)+r^2(-1+2ar^2\zeta))^2} \\
& + \frac{2r^2\left(-\frac{2L^2\alpha}{(L^2+r^2)^2} - 2a(1+\alpha)\zeta - \frac{(L^2+r^2)^3\beta(-1+2a(L^2+2r^2)\zeta)}{(L^2(-3+2ar^2\zeta)+r^2(-1+2ar^2\zeta))^2} + \frac{3(L^2+r^2)^2\beta}{L^2(-3+2ar^2\zeta)+r^2(-1+2ar^2\zeta)}\right)}{L^4\left(1+\frac{r^2}{L^2}\right)} \\
& - \left. \frac{r^2\left(\frac{2L^2\alpha}{L^2+r^2} - (1+\alpha)(-1+2ar^2\zeta) + \frac{(L^2+r^2)^3\beta}{L^2(-3+2ar^2\zeta)+r^2(-1+2ar^2\zeta)}\right)^2}{L^6\left(1+\frac{r^2}{L^2}\right)^2} \right].
\end{aligned} \tag{3.39}$$

In order for the relativistic stellar model to be physically acceptable, the speed of sound within its interior must be lower than the speed of light in both the radial and transverse directions. This can be expressed as $0 < v_r^2, v_t^2 < 1$. The idea of "cracking" was developed by Herrera [32] for the anisotropic distribution of materials. Later on, Abreu et al. [33], using the "cracking" notion, established that the region is possibly stable where $-1 < v_t^2 - v_r^2 < 0$ and potentially unstable where $0 < v_t^2 - v_r^2 < 1$ inside the anisotropic fluid sphere. This implies $0 \leq v_t^2 - v_r^2 \leq 1$.

The graphical behaviors for our model are displayed in Figure (3.14) which allows us to comprehend that our model satisfies the causality condition and the area within the star is possibly stable. Both radial and tangential speeds of sound increase with the increase in radius.

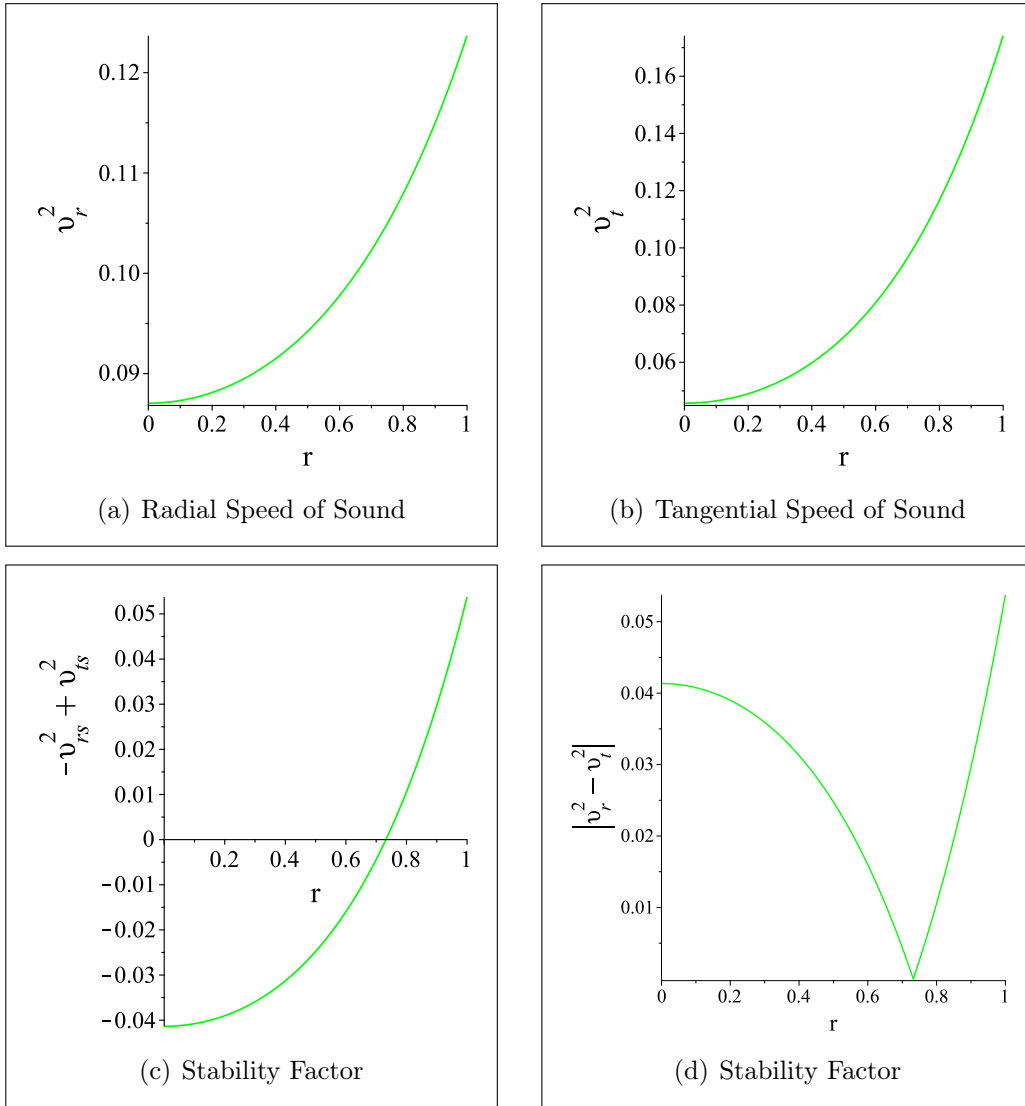


Figure 3.14: Graph of Radial and Tangential Speed of Sounds are plotted for the constants: $L = 1.8$, $a = 1.08977$, $\zeta = 0.01$, and $\alpha = 0.06184373$ with respect to r .

Energy Conditions

The energy conditions should be satisfied by the compact object in order to be physically feasible:

1. Weak Energy Condition (WEC): $p_r + \rho \geq 0$, $p_t + \rho \geq 0$,
2. Strong Energy Condition (SEC): $2p_t + p_r + \rho$,
3. Null Energy Condition (NEC): $\rho \geq 0$.
4. Dominant Energy Condition (DEC): $\rho - |p_r + 2p_t| \geq 0$. All energy conditions for our model are satisfied and graphs are shown in Figure (3.15).

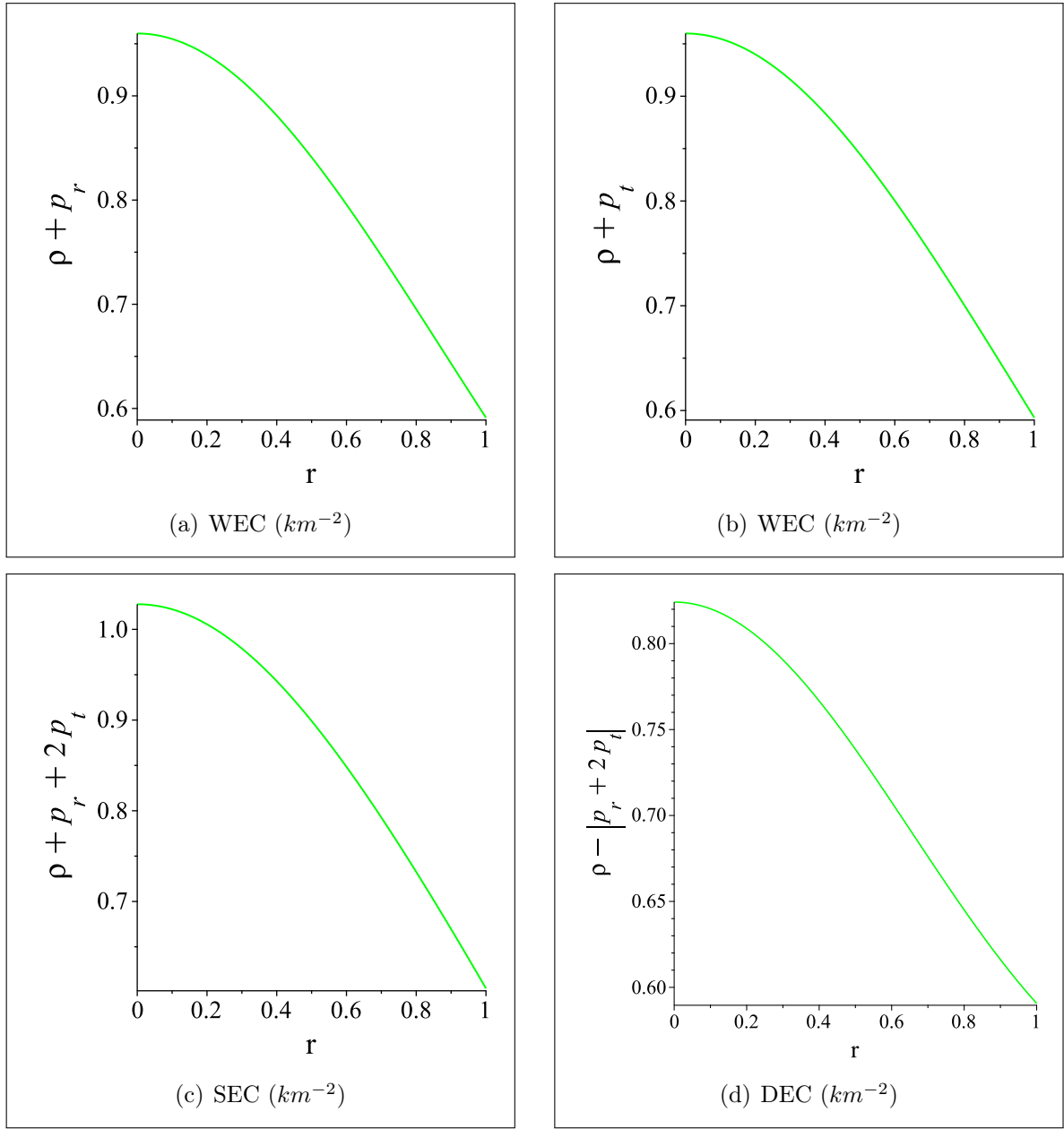


Figure 3.15: Graphs of Energy Conditions are plotted for the constants: $L = 1.8$, $a = 1.08977$, $\zeta = 0.01$, and $\alpha = 0.06184373$ with respect to r .

Adiabatic Index

Two specific heat ratios as stated by Heintzmann and Hillebrandt [34] and Chan et al. for the stable system is [35]

$$\Gamma_r = \frac{\rho + p_r}{p_r} \frac{dp_r}{d\rho}, \quad (3.40)$$

$$\Gamma_t = \frac{\rho + p_t}{p_t} \frac{dp_t}{d\rho}. \quad (3.41)$$

The model is said to be physically acceptable if the value of both adiabatic indices is greater than $\frac{4}{3}$. For our model this condition is satisfied and graphs of the adiabatic index are shown in Figure (3.16). With the increasing r both adiabatic indices show the

increasing behavior. The higher values of adiabatic indices towards the boundary increase the stability of the compact star.

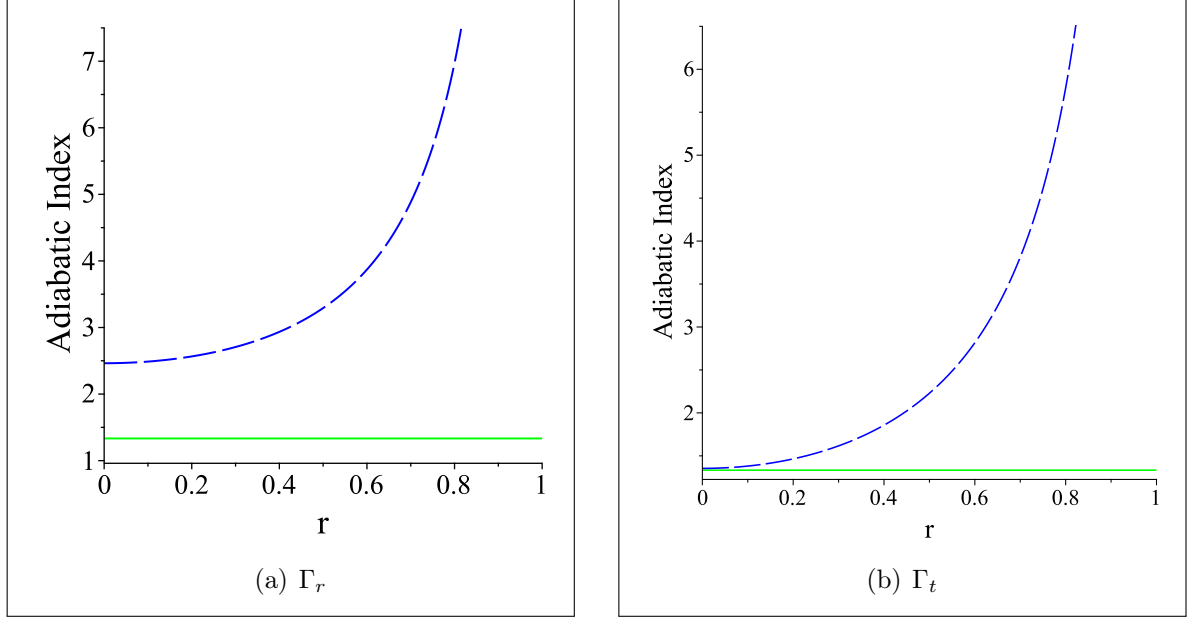


Figure 3.16: Graph of Radial and Tangential Adiabatic Index are plotted for the constants: $L = 1.8$, $a = 1.08977$, $\zeta = 0.01$, and $\alpha = 0.06184373$ with respect to r .

State of Equilibrium Under Different Forces

If the equation derived by Tolman-Oppenheimer-Volkoff in references [36] and [37] is met, then the star system is regarded as being in a condition of equilibrium. It is also known as TOV equation, given as

$$\frac{2}{r}(p_t - p_r) - \frac{dp_r}{dr} - (\rho + p_r)\nu' + \sigma E e^\lambda = 0 \quad (3.42)$$

Eq (3.42) can be written as

$$F_a + F_h + F_g + F_e = 0 \quad (3.43)$$

Where, F_a , F_h , F_e , and F_g are anisotropic, hydrostatic, electric, and gravitational forces respectively, given as

$$F_a = \frac{2}{r}(p_t - p_r), F_h = -\frac{dp_r}{dr}, F_e = \sigma E e^\lambda, F_g = -(\rho + p_r)\nu'.$$

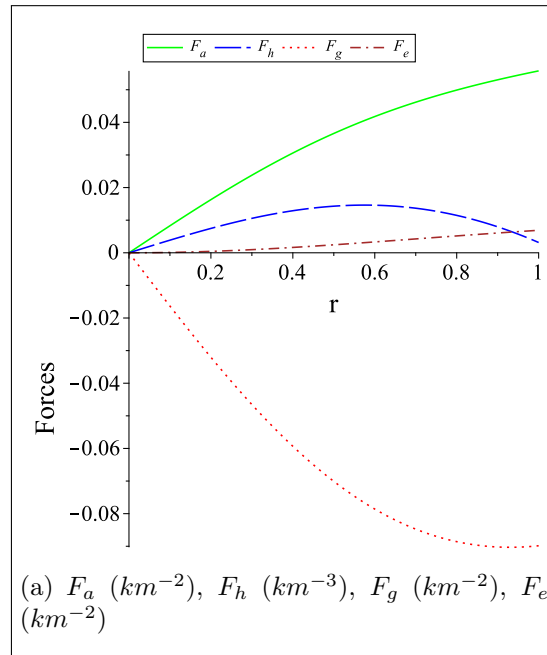


Figure 3.17: Graph of Forces is plotted for the constants: $L = 1.8$, $a = 1.08977$, $\zeta = 0.01$, and $\alpha = 0.06184373$ w.r.t r . Where, the green curve depicts the anisotropic force, the blue dashed curve represents the hydrostatic force, the brown dashed curve represents the electric force, and the red dotted curve represents the gravitational force.

Chapter 4

Conclusion

This thesis investigates exact solutions to Einstein's field equations in paraboloidal geometry using Chaplygin's equation of state. The work has extended the knowledge of compact objects by including charged anisotropic model affected by a Chaplygin gas equation. Einstein's field equations are developed for a spacetime that exhibits spherical symmetry using paraboloidal coordinates. We are able to simplify these equations and derive exact solutions by using Chaplygin's equation of state. The model proposed in this thesis has potential implications for understanding the behavior of compact objects, such as neutron stars and quark stars, under extreme conditions. Chaplygin's equation of state, which contains both fluid and exotic matter features, offers a useful tool for describing such phenomena. To verify the physical viability of the solutions, a thorough analysis was conducted. Within the interior of the compact object, the energy density, radial pressure, and tangential pressure were found to be regular and well-behaved. Moreover, the solutions meet the essential energy requirements, demonstrating the stability and physical feasibility of the model. The inclusion of charge and anisotropy was shown to have significant effects on the properties of the compact object. The charged anisotropic model demonstrated different properties compared to their uncharged and isotropic counterparts, providing greater insights into the structure and behavior of such celestial objects. The solutions produced in this study were compared with known precise solutions in different geometries. Our results were consistent with previous literature, indicating the stability and correctness of our technique in the setting of paraboloidal geometry.

Bibliography

- [1] Sachs, M. (1996). Changes in concepts of time from Aristotle to Einstein. *Astrophysics and Space Science*, 244, 269-281.
- [2] Faraoni, V. (2013). *Special Relativity*. New York, NY: Springer.
- [3] Klein, M. J. (1961). Max Planck and the beginnings of the quantum theory. *Archive for History of Exact Sciences*, 1, 459-479.
- [4] Puri, S. P. (2013). *General theory of Relativity*. Pearson Education India.
- [5] Maxwell, J. C. (1865). VIII. A dynamical theory of the electromagnetic field. *Philosophical transactions of the Royal Society of London*, (155), 459-512.
- [6] Griffiths, D. J. (2023). *Introduction to Electrodynamics*. Cambridge University Press.
- [7] D’Inverno, R. A., & Einstein, A. (1992). *Introduction Einstein’s Relativity*. Clarendon Press.
- [8] MICHELSON, A., & MORLEY, E. (1991). On the relative motion of the earth and the luminiferous ether. *SPIE milestone series*, 28, 450-458.
- [9] Einstein, A. (1905). On the electrodynamics of moving bodies. *Annalen der Physik*, 322(10), 891-921.
- [10] Einstein, A. (1922). The general theory of relativity. In *The meaning of relativity* (pp. 54-75). Dordrecht: Springer Netherlands.
- [11] Hobson, M. P., Efstathiou, G. P., & Lasenby, A. N. (2006). *General Relativity: An Introduction for Physicists*. Cambridge University Press.
- [12] Bambi, C. (2018). *Introduction to general relativity: a course for undergraduate students of physics*. Springer.
- [13] MacCallum, M. A. (2006, June). Finding and using exact solutions of the Einstein equations. In *AIP Conference Proceedings* (Vol. 841, No. 1, pp. (129-143). American Institute of Physics.
- [14] Bunney, C. R., & Gradoni, G. (2021). Electromagnetism in curved space-time: Coupling doppler shifts and gravitational redshifts. *IEEE Antennas and Propagation Magazine*, 64(3), 40-51.
- [15] Stephani, H., Kramer, D., MacCallum, M., Hoenselaers, C., & Herlt, E. (2009). *Exact solutions of Einstein’s field equations*. Cambridge university press.

- [16] Carroll, S. M. (2019). Spacetime and geometry. Cambridge University Press.
- [17] Mussa, A. (2014). Spherical symmetry and hydrostatic equilibrium in theories of gravity (Doctoral dissertation, UCL (University College London)).
- [18] Camenzind, M. (2007). Compact objects in astrophysics (pp. 1-25). Springer Berlin Heidelberg.
- [19] Schwarzschild, K. (2003). On the gravitational field of a mass point according to Einstein's theory. *Gen. Relativ. Gravit*, 35(5), 951-959.
- [20] Reissner, H. (1916). Über die Eigengravitation des elektrischen Feldes nach der Einsteinschen Theorie. *Annalen der Physik*, 355(9), 106-120.
- [21] Nordström, G. (1918). On the energy of the gravitation field in Einstein's theory. *Koninklijke Nederlandse Akademie van Wetenschappen Proceedings Series B Physical Sciences*, 20, 1238-1245.
- [22] Chandrasekhar, S., & Chandrasekhar, S. (1957). *An Introduction to the Study of Stellar Structure* (Vol. 2). Courier Corporation.
- [23] Pandey, S. C., Durgapal, M. C., & Pande, A. K. (1991). Relativistic polytropic spheres in GR. *Astrophysics and Space Science*, 180, 75-92.
- [24] Kippenhahn, R., Weigert, A., & Weiss, A. (1990). *Stellar structure and evolution* (Vol. 192). Berlin: Springer-Verlag.
- [25] Thirukkanesh, S., Sharma, R., & Das, S. (2020). Model of a static spherically symmetric anisotropic fluid distribution in paraboloidal spacetime admitting a polytropic equation of state. *The European Physical Journal Plus*, 135(8), 1-14.
- [26] Karmakar, S., Mukherjee, S., Sharma, R., & Maharaj, S. D. (2007). The role of pressure anisotropy on the maximum mass of cold, compact stars. *Pramana*, 68, 881-889.
- [27] Thomas, V. O., & Pandya, D. M. (2017). Anisotropic compact stars on paraboloidal spacetime with linear equation of state. *The European Physical Journal A*, 53(6), 120.
- [28] L'DOVICH, Y. B. Z. (1962). The equation of state at ultrahigh densities and its relativistic limitations. *Soviet Physics JETP*, 14(5).
- [29] Bondi, S. H. (1999). The gravitational redshift from static spherical bodies. *Monthly Notices of the Royal Astronomical Society*, 302(2), 337-340.
- [30] Buchdahl, H. A. (1959). General relativistic fluid spheres. *Physical Review*, 116(4), 1027.
- [31] Thorne, K. S., Misner, C. W., & Wheeler, J. A. (2000). *Gravitation*. San Francisco: Freeman.
- [32] Herrera, L. (1992). Cracking of self-gravitating compact objects. *Physics Letters A*, 165(3), 206-210.

- [33] Abreu, H., Hernández, H., & Núñez, L. A. (2007). Sound speeds, cracking and the stability of self-gravitating anisotropic compact objects. *Classical and Quantum Gravity*, 24(18), 4631.
- [34] Heintzmann, H., & Hillebrandt, W. (1975). Neutron stars with an anisotropic equation of state-mass, redshift and stability. *Astronomy and Astrophysics*, vol. 38, no. 1, Jan. 1975, p. 51-55. Research supported by the Deutsche Forschungsgemeinschaft., 38, 51-55.
- [35] Chan, R., Herrera, L., & Santos, N. O. (1993). Dynamical instability for radiating anisotropic collapse. *Monthly Notices of the Royal Astronomical Society*, 265(3), 533-544.
- [36] Tolman, R. C. (1939). Static solutions of Einstein's field equations for spheres of fluid. *Physical Review*, 55(4), 364.
- [37] Oppenheimer, J. R., & Volkoff, G. M. (1939). On massive neutron cores. *Physical Review*, 55(4), 374.
- [38] Delgaty, M. S. R., & Lake, K. (1998). Physical acceptability of isolated, static, spherically symmetric, perfect fluid solutions of Einstein's equations. *Computer Physics Communications*, 115(2-3), 395-415.
- [39] Gokhroo, M. K., & Mehra, A. L. (1994). Anisotropic spheres with variable energy density in GR. *General relativity and gravitation*, 26, 75-84.
- [40] Herrera, L. (2020). Stability of the isotropic pressure condition. *Physical Review D*, 101(10), 104024.
- [41] Maurya, S. K., & Tello-Ortiz, F. (2019). Generalized relativistic anisotropic compact star models by gravitational decoupling. *The European Physical Journal C*, 79, 1-14.
- [42] Feroze, T., & Siddiqui, A. A. (2011). Charged anisotropic matter with quadratic equation of state. *General Relativity and Gravitation*, 43, 1025-1035.
- [43] Bhar, P., Govender, M., & Sharma, R. (2018). Anisotropic stars obeying Chaplygin equation of state. *Pramana*, 90, 1-9.
- [44] Ragel, F. C., & Thirukkanesh, S. (2019). General relativistic model for mixed fluid sphere with equation of state. *The European Physical Journal C*, 79(4), 306.
- [45] Kumar, M., & Kumar, J. (2023). Model for anisotropic compact stars via Chaplygin equation of state in Tolman space-time. *Physica Scripta*, 98(3), 035012.